

12-2010

RMI1 is Essential for Early Embryonic Development and Attenuation of Tumor Development

Haoyi Chen

Follow this and additional works at: https://digitalcommons.library.tmc.edu/utgsbs_dissertations



Part of the [Molecular Genetics Commons](#)

Recommended Citation

Chen, Haoyi, "RMI1 is Essential for Early Embryonic Development and Attenuation of Tumor Development" (2010). *The University of Texas MD Anderson Cancer Center UTHealth Graduate School of Biomedical Sciences Dissertations and Theses (Open Access)*. 94.

https://digitalcommons.library.tmc.edu/utgsbs_dissertations/94

This Dissertation (PhD) is brought to you for free and open access by the The University of Texas MD Anderson Cancer Center UTHealth Graduate School of Biomedical Sciences at DigitalCommons@TMC. It has been accepted for inclusion in The University of Texas MD Anderson Cancer Center UTHealth Graduate School of Biomedical Sciences Dissertations and Theses (Open Access) by an authorized administrator of DigitalCommons@TMC. For more information, please contact digitalcommons@library.tmc.edu.

RMI1 Is Essential for Early Embryonic Development and Attenuation of Tumor Development

By

Haoyi Chen, B.S.

APPROVED:

Lei Li, Ph.D.

Supervisory Professor

Andreas Bergmann, Ph.D.

Mong-Hong Lee, Ph.D.

Randy J. Legerski, Ph.D.

Guillermina Lozano, Ph.D.

APPROVED

George M. Stancel, Ph.D.

Dean, the University of Texas
Health Science Center at Houston
Graduate School of Biomedical Sciences

RMI1 Is Essential for Early Embryonic Development and Attenuation of Tumor Development

**A
DISSERTATION**

**Presented to the Faculty of
The University of Texas
Health Science Center at Houston
And The University of Texas
M. D. Anderson Cancer Center
Graduate School of Biomedical Sciences
In Partial Fulfillment
Of the Requirements
For the Degree of
DOCTOR OF PHILOSOPHY**

**By
Haoyi Chen, B.S.
Houston, Texas
December, 2010**

DEDICATION

This dissertation is dedicated to my wife, Yingjun Jiang,
And daughter, Stephanie Chen.

ACKNOWLEDGEMENTS

I would first like to thank my mentor, Dr. Lei Li, for his continuous encouragements, instructions and patience during the last six years. His passion and enthusiasm towards Biology and his profession has always been, and will continue to be my inspiration and motivation in my future careers.

I would also like to thank my past and current committee members: Dr. Andreas Bergmann, Dr. Mong-Hong Lee, Dr. Randy Legerski, Dr. Guillermina Lozano, Dr. Pierre McCrea, Dr. Bing Su and Dr. Michael Van Dyke. Valuable help, suggestions and advice provided from my committee members have made a great difference in my research project and helped keep it on right direction.

I am also indebted to Dr. Xin Wang, Dr. Xi Shen, Dr. Yucai Wang, Yaling Huang, and all the staff members in Dr. Lei Li's lab for their help in experiments. Especially, I want to thank Dr. Chang Xu, a formal Ph.D student from our lab, for her excellent pioneer research in RMI1 gene and invaluable suggestions in my project.

I appreciate supports from GSBS and department of Experimental Radiation Oncology.

Finally, I would sincerely thank my family members for their everlasting encouragements, patience and goodwill. My special thanks to my daughter Stephanie and wife Dr. Yingjun Jiang, who recently graduated from GSBS.

RMI1 Is Essential for Early Embryonic Development and Attenuation of Tumor Development

Publication No.

Haoyi Chen

Supervisory Professor: Lei Li, Ph.D.

Abstract

RMI1 (BLM-Associated Protein 75 or Blap75) is highly conserved from yeast to human. Previous studies have shown that hRMI1 is required for BLM/TopoIII α /RMI1 complex stability and function. However, in vivo functions of RMI1 remain elusive. To address this question, I generated RMI1 knockout mice by homologous replacement targeting. While RMI1 $^{+/-}$ mice showed no obvious phenotype, deletion of both RMI1 alleles leads to early embryonic lethality before implantation. I then generated RMI1/p53 double knockout mice. After ionizing radiation treatment at 4Gy, RMI1/p53 double-heterozygous mice showed shortened tumor latency and aggressive tumor types when comparing with wild type, RMI1 $^{+/-}$ and p53 $^{+/-}$ control cohorts. My study suggests a dual-functional role of RMI1 in early embryonic development and tumor suppression.

Table of Contents

Approval Page.....	i
Title Page.....	ii
Dedication.....	iii
Acknowledgements.....	iv
Abstract.....	vi
Table of Contents.....	vii
List of Illustrations.....	xii
List of Tables.....	xiv

Chapter I. Introduction and Significance

Introduction of BLM.....	1
BLM mutants cause Bloom syndrome (BS)	1
BLM belongs to RecQ DNA helicase family	2
Structure feature and biochemical activity of BLM protein.....	6

Biological function of BLM.....	10
The BTB complex.....	22
Components of BTB complex.....	22
Introduction of Topo3 α	23
Introduction of Rmi1.....	25
Introduction of RMI2.....	27
Activity of BTB complex.....	28
Mouse models of BTB complex proteins.....	33
Mouse models of BLM.....	33
Mouse model of Topo3 α	34
Potential application of RMI1 mouse model.....	34

Chapter II. RMI1 Is Required for Early Embryonic Development

Material and Methods.....	36
Identification and cloning of mRMI1 gene and full-length cDNA.....	36
Generation of mouse RMI1 knockout construct.....	37
Identification of Rmi1 mouse ES cell clones.....	39

Germline transmission.....	40
Southern blot tests form ES cell genotyping.....	41
PCR for mice and embryo genotyping.....	41
Cell culture and Clonogenic survival assay.....	43
Results.....	44
Generation of RMI1 Knockout Mouse Model.....	44
Embryonic Lethality of RMI1 ^{-/-} Mice.....	47
P53-dependent Cell Proliferation in RMI1-depleted Cell.....	50
p53 ^{-/-} did not alleviate early embryonic lethality of RMI1 ^{-/-} mice.....	51
Discussion.....	54
RMI1 is essential for early embryonic development.....	54
Functional relationship of Rmi1 and p53.....	56

Chapter III. RMI1 Heterozygosity Accelerates Induced-tumor Formation of p53^{+/-} Mice

Materials and Methods.....	58
Ionizing radiation treatment and tumor analysis of animal model.....	58
Genomic DNA extraction from fixed specimens.....	59

Preparation MEF cells.....	59
Immuno-staining of radiation-induced foci.....	60
Results.....	61
Shortened half-life of radiation-induced foci in p53 ^{+/-} RMI1 ^{+/-} MEFs.....	61
Ionizing radiation fails to induce enhanced tumor formation in RMI1 ^{+/-} mice.....	62
Rmi1 heterozygosity accelerates IR-induced tumor formation of p53 ^{+/-} mice.....	67
LOH assays on RMI1 and p53 loci.....	72
Discussion.....	78
Functional relationship between p53 and RMI1.....	78
Recessive haploinsufficiency of RMI1 ^{+/-} mice.....	79
Potential clinic application of RMI1 mouse model.....	82
 Chapter IV. Conclusion and Future Directions	
Conclusion.....	84
Future Direction.....	84
Study molecular modification of RMI1.....	85
Study functional domains of RMI1.....	86
Study potential protein partners of RMI1.....	87

Study RMI1 mutations/SNP in human cancers.....	87
Bibliography.....	89
 Appendix I Interactions of INO80 Complex Subunits	
Introduction & Significance.....	103
Classification of chromatin remodeling complexes.....	103
Cellular functions of INO80 complex.....	109
Protein Components of INO80 Complex.....	112
Bimolecular fluorescence complementation assay.....	118
Goals of experiment.....	118
Materials and Methods.....	122
Cell Culture and cDNA Cloning/Transfection.....	122
Immunoblotting and Green Fluorescent Signal Detection.....	123
Results.....	124
Constructions and expressions of YFP-tagged INO80 subunits.....	124
Fluorescence microscopy	127
Discussion.....	132

Bibiliography	134
---------------------	-----

Appendix II Data Sheet of Irradiated Mice	138
--	-----

Vita	142
-------------------	-----

List of Illustrations

Chapter I, II, III & IV

Figure 1. Schematic of RecQ helicase family members from various organisms.....	3
Figure 2. Protein structure and map of interaction regions of BLM.	7
Figure 3. BLM prevents crossovers in DSB repair.	20
Figure 4. Model of BTB complex ‘dissolution’ activity.	31
Figure 5. Replacement targeting of the RIM1 locus.	45
Figure 6. Clonogenic survival assay of Rmi1 knockdown in HCT116 cells.	52
Figure 7. Foci staining 6, 24, and 48h after IR (1.5gy).....	63
Figure 8. Accelerated and enhanced IR-induced tumorigenesis in Rmi1 ^{+/-} p53 ^{+/-} mice.....	70
Figure 9. Aggressive tumors derived from the RMI1 ^{+/-} p53 ^{+/-} mice.	74
Figure 10. LOH assay of RMI1 and p53 loci.	76

Appendix I

Figure 1. Known domains and interactions of Ino80 protein.	115
--	-----

Figure 2. Principle of BiFC assay.	120
Figure 3. Western blots for YFP fragments tagged INO80 complex subunits.	125
Figure 4. Fluorescent microscopy of BiFC assay	128

List of Tables

Chapter I, II, III & IV

Table 1. Summary of embryonic genotypes.48

Table 2. Summary of foci-negative MEF populations 24 or 48 hours after IR.....65

Table 3. Summary of induced-tumors from Rmi1^{+/-} p53^{+/-} and control groups.68

Appendix I

Table 1. List of covalent histone modifications.105

Table 2. List of ATP-dependent chromatin remodeling complexes.107

Table 3. Subunits of budding yeast and human INO80 complexes.113

Table 4. summary of protein-protein interactions among INO80 complex subunits
identified by BiFC assay.....130

Chapter I

Introduction & Significance

1.0 Introduction of BLM

1.1 BLM mutants cause Bloom syndrome (BS)

Bloom syndrome (BS) is a rare autosomal recessive disorder. Since first described in 1954, more than 170 cases of BS patients have been reported. One of the major clinical features of Bloom syndrome is the high frequency of cancers at early ages. Moreover, in contrast to other cancer-prone disorders such as Fanconi anemia (FA) or Ataxia telangiectasia (AT) (1, 2), BS patients are exposed to a much broader spectrum of malignancies, which includes almost all types of cancers affecting the

general population. Additional features of this syndrome include dwarfism, sun light sensitivity, male infertility, and immunodeficiency (3).

BS is caused by defects in the BLM (Bloom Syndrome Mutated) gene. Until recently, at least 64 different BLM mutations derived from BS patients have been identified (4, 5). Most mutations are nonsense or frame-shift ones that cause premature protein-translation termination. Missense contributes up to 16% of total BS-associated mutations (4). Among all known mutations, BLM^{Ash}, first identified from Ashkenazi Jews population which bears the highest risk of BS, corresponds to a 6-bp deletion and a 7-bp insertion at position 2207 (6). Interestingly, unlike most other recessive disorders, the BLM^{Ash} allele is reported to be haploinsufficient. Carriers of one copy BLM^{Ash} allele are exposed to an increased risk of colorectal cancer (7, 8).

1.2 BLM belongs to RecQ DNA helicase family

BLM belongs to RecQ DNA helicase family (**Figure 1.**), a member of SF2 helicase superfamily (9). RecQ helicases are highly conserved from bacteria to humans. Helicases from this family contain a conserved helicase domain consisted of seven characteristic sequence motifs (10). In addition, most RecQ helicases present other conserved domains, including the RQC (RecQ C-terminal) and HRDC (helicase and RNase D C-terminal) domains (11, 12).

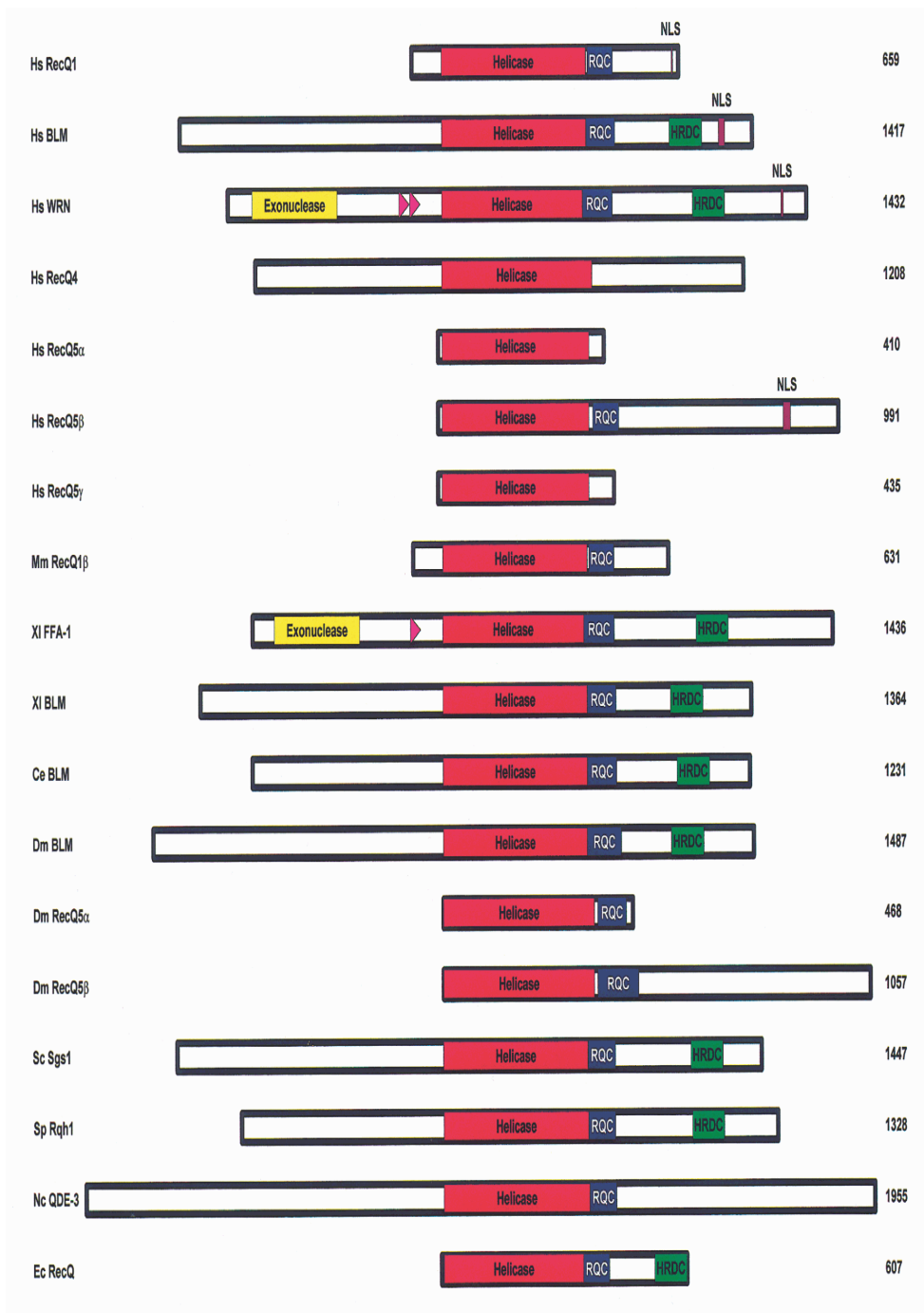


Figure 1. Schematic of RecQ helicase family members from various organisms. Left: the names of proteins and organisms (Hs, *Homo sapiens*; Mm, *Mus musculus*; Xl, *Xenopus laevis*; Ce, *Caenorhabditis elegans*; Dm, *Drosophila melanogaster*; Sc, *Saccharomyces cerevisiae*; Sp, *Schizosaccharomyces pombe*; Nc, *Neurospora crassa*; Ec, *Escherichia coli*). Middle: schematic representations of RecQ helicases (red, blue and green: conserved domains of helicase, RQC and HRDC, respectively; yellow: exonuclease domain; purple: NLS sequence; pink: unique repeat in FFA-1). Right: the sizes of proteins (number of amino acids). Adapted from Csana and Z. Bachrati and Ian D. Hickson, RecQ helicases: suppressors of tumorigenesis and premature aging., *Biochemical Journal* (2003) Volume **374**, 577-606

The number of RecQ helicases in different species varies. It seems that this number is associated with organism complexity. Whereas *Escherichia coli* and *Saccharomyces cerevisiae* only contain a single RecQ helicase (RecQ and Sgs1, respectively), human cell expresses at least five of the RecQ family members: RECQL1, RECQL4, RECQL5, WRN, and BLM (9).

Besides BLM, mutations of some of the other human RecQ helicases also lead to genetic disorders. For example, mutations in the RECQL4 and WRN gene cause Rothmund-Thomson syndrome and Werner syndrome, respectively (13, 14). Both syndromes are manifested by predisposition of cancers. However, unlike BS patients who have increased susceptibility to a wide spectrum of cancers, patients of Rothmund-Thomson or Werner syndrome are prone to certain types of cancers, such as osteosarcoma and thyroid cancers, respectively.

Previous studies have shown that all RecQ helicases possess several common enzymatic activities, such as: 1) DNA- and Mg^{2+} -dependent ATPase activity; 2), 3' to 5' DNA helicase activity (with the exception of RECQL4 (15)); 3) complementary single strand DNA annealing; 4) Branch migration of Holiday Junctions; 5) replication fork regression. However, although human RecQ helicases, especially BLM and WRN, have similar biochemical activities, and their defective cells both display chromosomal integrity related phenotypes, their functions are mostly non-redundant (9).

1.3 Structure feature and biochemical activity of BLM protein

The hBLM protein comprises 1417 amino acids. As previously described in this chapter, BLM contains several conserved domains common in RecQ helicase family, including a central SF2 helicase domain of repeat motifs, a RQC (RecQ C-terminal) and a HRDC helicase and RNase D C-terminal) domain (**Figure 2.**).

Among them, the helicase domain possesses both DNA helicase and ATPase activity. The RQC domain, on the other hand, forms a zinc-binding scaffold, which is required for this protein's structural stability. Moreover, the winged-helix (WH) sub domain of RQC domain is response for DNA binding (16). The third conserved domain of BLM, the HRDC domain is indispensable for the efficient binding and unwinding activities of double Holliday junctions (17). Taking together, all of three domains are important in terms of proper BLM activity, as disease-causing mutations in all three domains have been found in BS patients.

Consistent with activities of its RecQ helicase homologs, BLM is able to recognize and unwind a wide variety of DNA substrates. These substrates include, but not limit to DNA structures depicting replication forks (forked duplex), replication obstacles (G-quadruplex), and recombination intermediates (Holliday junctions, D-loops) (18-20). The capability of unwinding such DNA substrates suggests that BLM is likely involved in cellular events of DNA metabolism, such as DNA replication, repair and telomere

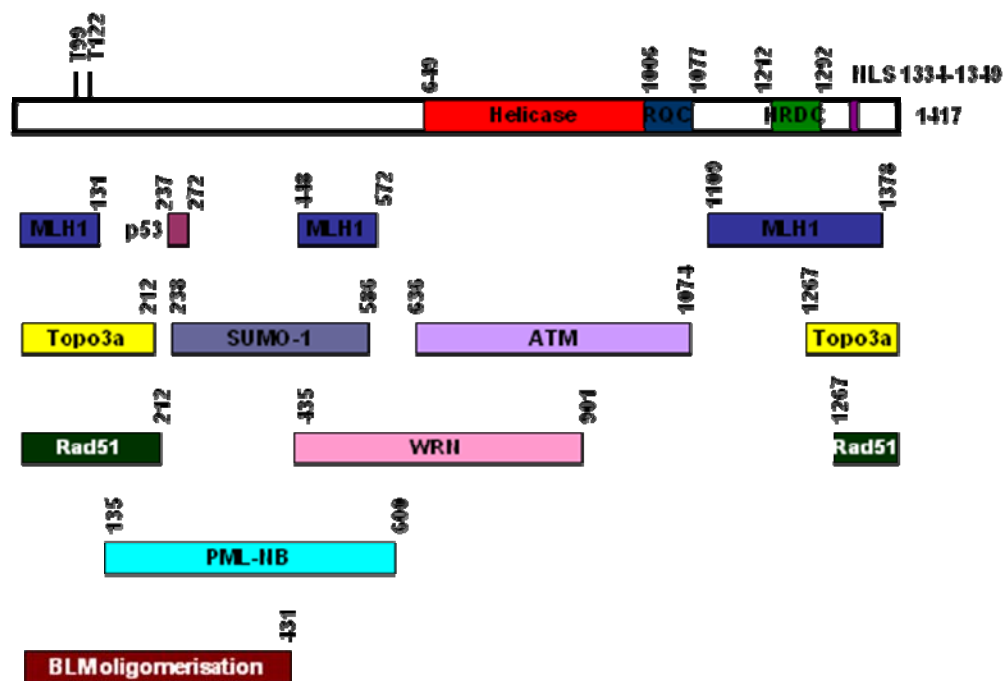


Figure 2. Protein structure and map of interaction regions of BLM. Conserved domains are labeled with colors in box depicting BLM protein. Color boxes below represent protein-protein interaction regions. The amino acid positions are listed for each domains, regions and phosphorylation sites. Adapted and modified from Csanad Z. Bachrati and Ian D. Hickson, RecQ helicases: suppressors of tumorigenesis and premature aging., *Biochemical Journal* (2003) Volume **374**, 577-606

maintenance. Interestingly, blunt-ended dsDNA, which represents normal DNA structure, is not a substrate of BLM (18). Moreover, BLM is proposed to have a 'reversed' helicase activity by catalyzing complementary ssDNA annealing (10).

The hallmark feature of cells derived from BS patients is the elevated Sister Chromatin Exchange (SCE) level, which still serves as the only objective criterion for BS diagnosis (5). The elevated SCE level could also be observed from mouse BLM^{-/-} cells, and BLM^{-/-} DT40 cells(21-23). SCE is the process that two sister chromatids physically exchange duplex strands by breaking and rejoining DNA chains (24). Although this process does not involve alternation of genetic information, and is generally considered to be conservative and error-free, elevated SCE level may be associated with increased risk of cancers (25). Because reciprocal interchange of SCE is carried by homologous recombination (HR) pathway, the SCE therefore represents, at least indirectly, the cellular HR activity. The fact that the SCE level of BS cells is approximately 10-fold higher than wild type cells indicates BLM function in preventing chromatid exchanges (21). Along with elevated SCE level, BLM-defective cells displayed increased frequency of gene targeting efficiency, loss of heterozygosity (LOH) rate, accumulated chromosome aberrations and IR-sensitivities (26-29). Conclusively, BLM is believed to play an important role in maintaining genomic stability and chromosomal integrity.

1.4 Biological function of BLM

For the last two decades or so, functions of BLM have been extensively investigated. Although the exact mechanisms remain obscure, it is widely accepted that BLM involves multiple cellular processes related to DNA metabolism. These processes include DNA replication in S phase, chromatin separation in M phase, DNA-damage response checkpoint regulation and DNA repair.

1.4.1 BLM function in DNA replication

1.4.1.1 Importance of DNA replication

DNA replication is the fundamental process for biological inheritance. The efficiency and fidelity of replication is critical for all eukaryotes. During replication, the replicated chromosome is unwound by DNA helicases, which leaves two single stranded DNA branching open and complemented by newly synthesized DNA. This particular Y-shaped DNA structure is termed replication fork. In normal situations, DNA replication starts with origins when two DNA strands are separated in order to form two replication forks proceeding in opposite directions, and ends when all forks meet and terminate (30). However, replication forks could be stalled by various reasons, such as encountering DNA breaks and defects (31-33). If not rescued,

failed replication forks would lead to interrupted replication process, stalled cell cycle or even cell death.

1.4.1.2 BLM helps to restart stalled replication forks during S phase.

The cellular expression of BLM protein is tightly regulated in cell type- and tissue-specific manners. In general, BLM expresses in all actively dividing cells with active cell proliferation. Therefore, testis, ovary, thymus and spleen are the organs that have the highest levels of BLM expression (23). Surprisingly, despite its function in maintaining genomic stability, most tumor cells express BLM at higher levels, presumably in keeping with the faster cell proliferation (34).

BLM expression is also temporally regulated as a function of the cell cycle (35-37). The BLM protein is abundant in both S and G2, but absent in the G1 phases. It is believed that proteolytic degradation after M phase leads to the undetectable BLM protein level in G1 phase (37), although direct evidence remains to be uncovered.

Several evidences suggest an association between BLM and DNA replication process. First, cell cycle-specific expression pattern of BLM is consistent with cellular process of DNA replication, as the peak of BLM protein level occurs since S

phase. Second, during S phase, the nuclear location of BLM foci overlaps with PCNA in damage-induced sites, an indication of BLM's involvement in maintaining proper DNA replication (27). However, BLM has not been found to be a constitutive component of the replisome and does not directly involve in DNA replication process. Studies of BLM orthologue in yeast suggest that unstrained activity of Sgs1 is toxic for cells (38-40). In conclusion, BLM is not required for normal replication process.

Moreover, under normal conditions, BLM is localized in PML nuclear bodies (PML-NBs) (41). PML-NB is named after PML gene, which is originally identified as the site of translocations in acute promyelocytic leukaemia (42). Although direct interaction between BLM and PML is yet to be confirmed, the region targeting BLM to PML-NB localization had been mapped, as BLM^{Δ133-137} mutation failed to co-localize with PML-NBs (43). BLM localizes in PML-NBs together with some of its protein partners and other proteins involved in DNA metabolism. However, the function of this co-localization is still debatable. The co-localization of BLM and PML-NB is never complete (44, 45). Nevertheless, the localization of BLM to PML-NBs is not vital to BLM function. Although in PML-deficient cells, BLM is unable to concentrate into foci but spread uniformly in nucleoplasm (44), expression of mutant BLM with disturbed PML-NB colocalization capability corrects high SCE level in BS cells (45). It is very likely that PML-NBs serve as temporary storage sites for BLM proteins, where BLM can be shuttled to and from PML-NBs in a timely manner. This view is well supported by independent studies. For example, in response to DNA

hydroxyurea induced replication stress, BLM leaves PML-NBs and re-localizes to stalled replication forks (46).

Although the translocation of BLM from storage sites to stalled replication forks has been an acceptable dogma and BLM is also known to unwind G-quadruplexes as well as other DNA secondary structures that may present as roadblocks during replication, the mechanism of BLM in ensuring DNA replication remains elusive. Several hypotheses have been raised. Although different in details, they all propose BLM's function in restarting stalled replication forks.

One of the possible consequences of failing to restore collapsed replication forks is DSBs at damage sites, which may lead to inappropriate strand exchanges by the HR repair machinery (47, 48). It is believed that BLM is required for stabilization and subsequent restart of replication forks blocked by DNA lesions (49). Heller et al. proposed that BLM may help to obtain a configuration of nascent strands, a rate-limiting step in replication restart (50, 51). Another possible mechanism suggests that BLM promotes fork regression to 'chicken feet' formation at damage site, thus allows the replication machinery to use the nascent lagging strand as a template to bypass DNA lesion (52).

In summary, the presence of BLM in S phase helps to restart stalled replication forks, which prevent possible chromosome rearrangements promoted by collapsed replication forks, as one of its function in maintaining chromosomal integrity.

1.4.2 BLM in S phase checkpoint

1.4.2.1 Checkpoint pathway ensures proper cellular progresses.

Cells are most vulnerable during S phase in terms of generating replication-associated mutants. Any error in the replicative process, if not properly treated, may lead to more dangerous forms of lesions that could affect genomic integrity, or even cell viability (53). In response to replication stresses, the S phase checkpoint pathway acts to suppress the firing of replication origins before DNA lesions are removed. Thus, the S phase checkpoint mechanism is important for both replication fidelity and cell survival (54).

1.4.2.2 BLM in S phase checkpoint

Recent studies suggest that during S phase and in addition to its role in restarting stalled replication forks, BLM may also be involved in S phase checkpoint pathway (55). BLM is known to interact with multiple proteins participating in S phase checkpoint pathways. BLM interacts with BRCA1 and was also identified as a component of BASC complex, a multi enzyme complex containing BRCA1 and several other proteins such as MLH1, MSH2, MSH6, RFC, and ATM. This interaction seems to be DNA damage-associated, because the co-localization of

BLM and BRCA1 foci increases following HU treatment (56). The functional significance of this complex, however, remains to be demonstrated.

BLM has functional and physical interactions with other checkpoint/DNA damage signaling proteins such as the MRN complex, p53, γ -H2AX, ATR and ATM (46, 57, 58). During S phase, followed DNA damage agent introduction, BLM is rapidly recruited onto damaged sites and co-localizes with γ -H2AX (59). This translocation may allow BLM interacting with ATR, Chk1 and 53BP1, and facilitating accumulation of them and other checkpoint proteins onto the damaged sites (60). In the absence of BLM, this recruitment of multiple proteins to damage sites is either absent or delayed, indicating a BLM-associated S phase checkpoint pathway (57). Interestingly and surprisingly, BLM's role in this process may be non-catalytic, since the helicase-defective mutant of BLM is able to support the recruitment of the above checkpoint factors to the damage-induced foci (57),

1.4.3 BLM in telomere maintaining

In normal condition, telomeres are regulated by a special reverse transcriptase termed telomerase (61). Some human cell lines and primary tumor cells, however, maintain their telomeres using an alternative mechanism named alternative lengthening of telomeres (ALT) (62). TRF2, which is one of the key components of the telomere complex, is involved in this recombination-dependent telomere

maintenance (63). It forms heterodimer with TRF1, and both proteins are thought to be involved in regulating telomeric length (64, 65).

The physical interaction between BLM and TRF2 has been identified both *in vitro* and *in vivo* (66). Interestingly, the co-localization of BLM and TRF2 was only observed in ALT cells but not telomerase-proficient cells (66). Overexpressing BLM results in ALT cell-specific increases in telomeric DNA (67), which suggests that BLM promotes recombination-dependent amplification of telomeres in ALT cells.

1.4.4 BLM in M phase

BLM seems to be indispensable for faithful sister chromatids separation during M phase (68). Defective separation processes were observed from yeast Δ Sgs1 and *Drosophila* BLM^{-/-} cells (69). The same phenotype was also shown from BS cells. Comparing with cells ectopically expressing BLM protein, BLM-defective cells have higher frequency of anaphase bridges and lagging chromatins. Nevertheless, BLM localizes to anaphase bridges with its protein partners (70). It is suggested that BLM ensures chromatid separation by facilitating complete sister chromatid decatenation in anaphase.

1.4.5 BLM in HR

1.4.5.1 General introduction of HR

DNA double strand break (DSB) is one of the most severe DNA damages to cells (71). Improper repair of DSB could result in accumulated chromosomal aberrations, abnormal rearrangement of the genome, arrested cell cycle or even cell death (72). In mammalian cells, two distinct pathways, NHEJ and HR, are the two major repair mechanisms in response to DSBs (73). The NHEJ directly ligates, with minimum processing, two exposed chromosome ends together without the need of homologous DNA template (74). The HR, on the other hand, utilizes a homologous sequence as template to replicate the damaged part (75). Thus, it is understandable that cells exhibit dominating HR activity in S and G2 but not G1 phases. Since in S and G2 phases, sister chromatids are readily available as homologous templates for HR.

Following DSB formation, the exposed DNA ends are first resected by DNA exonuclease to release 3' single-strand overhangs. Next, these overhangs form a "presynaptic filament" with Rad51 and its paralogs, which leads to the invasion of a homologous region. During the invasion process, a 'D-loop' intermediate DNA structure is formed. After the strand invasion, DNA synthesis occurs on the invading strand to restore the broken chromosome. Another DNA

intermediate, Holliday junctions (HJs), are created during DNA synthesis. The HJs are proposed to be solved by DNA helicases, in either crossover or non-crossover manners (76, 77).

1.4.5.2 BLM function in HR

One of BS cell's characterized features is elevated SCE level, which indicates increased chromatid exchange activity in the absence of BLM protein. As discussed previously, the increased SCE level represents elevated HR activity in BS cells.

Previous studies suggest that BLM prevents this activity in two ways.

Simultaneously, it inhibits entry of cross over-causing HR and, during HR, it resolves DNA intermediates in a non-crossover manner (78, 79) (**Figure 4.**).

BLM displays anti-HR activity. It is widely recognized that the initial step of HR is the invasion of Rad51-coated ssDNA to homologous region (80). BLM can actively disrupt Rad51-ssDNA filaments. This disruption inhibits the invasion of homologous region and formation of 'D-loop' DNA intermediate (81). Since the Rad51 recruitment and strand invasion are the initial steps of HR, BLM could alter the repair mechanism from HR to non-cross over causing ones such as single strand annealing (SSA) or synthesis-dependent strand annealing (SDSA) (81).

On the other hand, BLM also plays a critical role in resolving DHJ intermediate. BLM, in coordination with its partner proteins Topo3 α and Rmi1, forms BTB complex (82). During the last steps of HR, this BLM-containing complex is capable of promoting HJ migration and dissociation in a non-crossover manner (20, 83). The components, structure and activity of BTB complex will be discussed in coming sections.

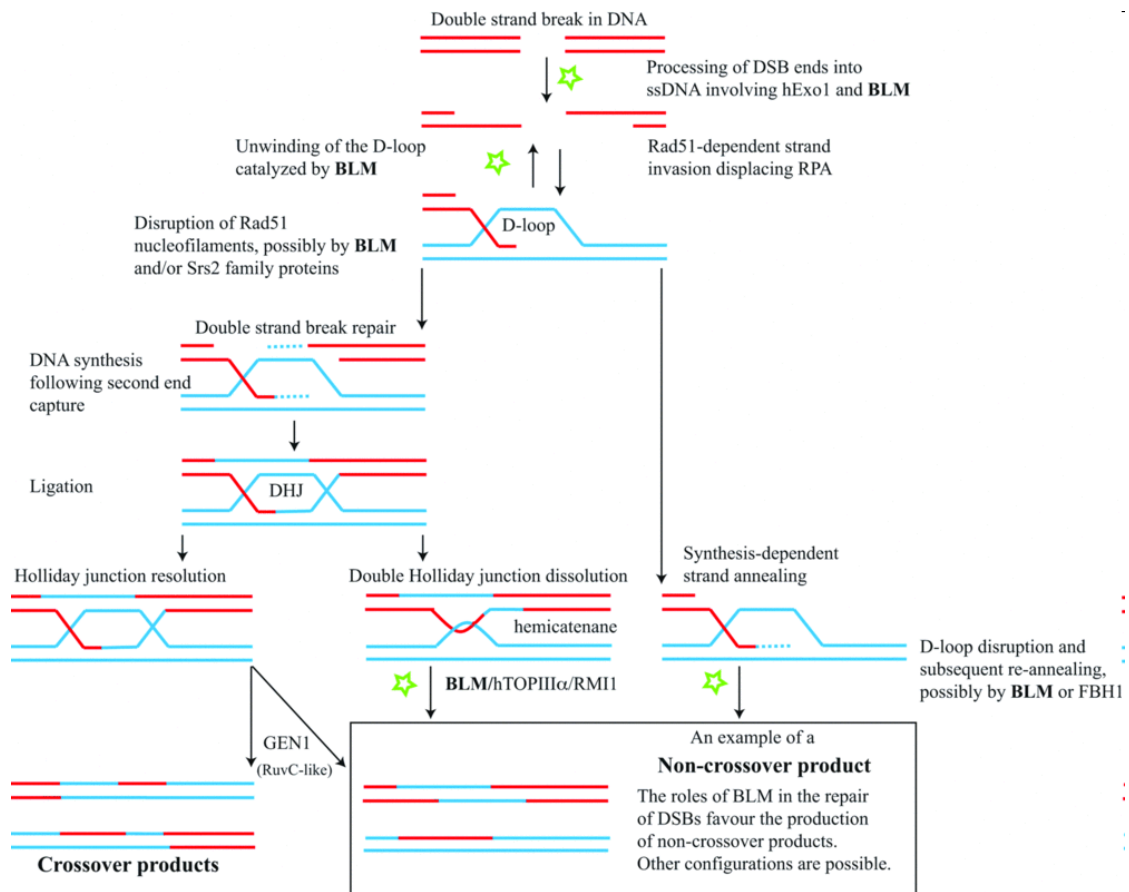


Figure 3. BLM prevents crossovers in DSB repair. BLM plays multiple roles in preventing chromatin exchanges caused by HR. BLM is able to re-direct DSB repair pathways from HR to SDSA by disrupting strand invasion process. It also leads to non-crossover dissolution of DHJs in HR. Adapted from Miranda Payne and Ian D. Hickson, Genomic instability and cancer: lessons from analysis of Bloom's syndrome., *Biochemical Society Transactions* (2009) 37, (553–559)

2.0 The BTB complex

2.1 Components of BTB complex

Three BLM-associated complexes, termed BLM complex I, II and III, have been isolated by Meeti et al. using biochemical purifications (84). Proteins from these complexes were identified by mass spectrometry. Most proteins identified have known physical interactions with BLM, including 5 Fanconi anemia (FA) proteins. Similar to BLM, defective FA proteins lead to genomic instability and show clinical features of cancer disposition (85). The fact that FA proteins and BLM co-exist as complexes may indicate a connection between the two pathways in maintaining genomic integrity (78).

Interestingly, only two proteins are consistently presented in all three BLM-associated complexes. They are the DNA topoisomerase Topo3 α and a newly identified novel protein Rmi1 (RecQ-mediated genomic instability 1, also named Blap75) (82). These two proteins, together with BLM, form a core complex termed BTB complex, referring to BLM, Topo3 α , and Rmi1 (Blap75). The formation of the BTB complex is conserved from yeast to human (86, 87). Recently, the fourth member of this complex, Rmi2 has been independently identified by two groups (88, 89). However, unlike all three other components of BTB complex, it only expresses in plants and vertebrates.

2.2 Introduction of Topo3 α

2.2.1 Topo3 α belong to type IA DNA topoisomerase subfamily

DNA topoisomerases are essential for almost all DNA metabolic processes, including compaction, replication, transcription, strand separation and recombination. All of these processes require exposing of accessible DNA helix (90, 91). DNA topological structures, which are generated during DNA metabolism, may be roadblocks in these processes. There are three main types of topology: supercoiling, knotting and catenation. DNA topoisomerases are able to break and reseal DNA backbones to facilitate topological changes and wind/unwind DNA. These enzymes could be structurally and mechanistically different. Based on the number of strands cut in one round of action, the majority of DNA topoisomerases can be separated into two families: type I and type II (90). Whereas the type I topoisomerase resolve topological structures by breaking and rejoining one strand of DNA helix, the type II topoisomerases act on both strands. The third DNA topoisomerase family, TopoV, is consisted of only one member (92).

Based on the polarity of strand cleavage, Type I topoisomerase family can be further divided into two subfamilies: IA and IB (93). The topoisomerases from type IA

subfamily are monomeric and able to unwind DNA substrates by breaking and sealing one DNA strand (94). The DNA helicase in the BTB complex, Topo3 α , belongs to type IA topoisomerase subfamily, which is conserved in all organisms.

2.2.2 Cellular function of Topo3 α

Function of Topo3 α remains poorly understood. Yeast top3 mutant strain shows phenotypes of hyper-recombination, slow growth, defective S phase checkpoint and abnormal sporulation (95-97). Interestingly, the phenotypes of top3 loss-of-function mutation can be suppressed by mutations in HR genes, or additional deletion of Sgs1, the only RecQ helicase in yeast (98-100), indicating a genetic interaction between Topo3 α and Sgs1.

Although Topo3 α is able to bind and unwind DNA substrates, its relaxation activity is weak. Thus it is believed that Topo3 α is not involved in the maintenance of DNA supercoiling homeostasis (101). However, it is required for proliferation and telomere stability in ALT (Alternative Lengthening of Telomeres) cells where Topo3 α physically interacts with TRF2 (102). Knockdown Topo3 α by siRNA induces TRF2 depletion, inhibited growth, anaphase bridge formation, and telomere dysfunction in such cells. Thus it is proposed that Topo3 α /BLM/TRF2 complex may be in response of maintaining telomere stability in ALT cells.

Topo3 α function is also associated with BLM and BTB complex. The activity of this complex as well as Topo3 α 's role will be discussed in section 2.5 of this chapter.

2.3 Introduction of Rmi1

2.3.1 Protein structures of RMI1

The hRmi1 harbors 625 amino acid residues and has a molecular weight of 75kDa (82). Examination of Rmi1 protein reveals three conserved domains: a DUF1767 (Domain of Unknown Function 1767, named by Genbank) and two OB-fold (Oligonucleotide/oligosaccharide-binding) domains (OB1 and OB2, respectively) (89). The exact function of DUF1767 domain remains unknown. Meanwhile, the two OB-fold domains share sequential similarities to OB-fold domains found in RecG and RPA1-C, respectively. Although OB-fold domain is generally considered as a DNA binding domain, the two domains in RMI1 lack several conserved residues that are important for DNA binding. Therefore it is predicted that Rmi1 has weak or no DNA binding activity. However, *in vitro* assays conducted by several groups lead to opposite results and the DNA binding activity of Rmi1 remains controversial (89, 103). It is still possible, however, that Rmi1 may bind DNA substrates only in the context of BTB complex. On the other hand, Rmi1 OB-fold domains may participate

in specific protein-protein interactions. A recent study has shown that OB1 and OB2 domains of Rmi1 are response for interactions with Topo3 α and Rmi2, respectively (89). A point mutation in OB1 domain disrupts Rmi1-Topo3 α interaction, and abolishes biochemical activity of BTB complex.

2.3.2 Function of RMI1

Previous studies from our lab and others have shown that Rmi1 is required for BTB complex stability and activity (82, 89). Rmi1 is required for normal cell proliferation. Rmi1 knockdown cells exhibit reduced cell density and drastic decrease in colony survival assay. Surprisingly, these cells do not display any sign of specific cell cycle arrest or apoptosis. One plausible explanation is that Rmi1 depletion leads to reduced proliferation. Rmi1 is also required for genomic stability. The Rmi1 knockdown cells display elevated SCE level, a characteristic feature of BS cells. The SCE level of Rmi1 knockdown cells is comparable to that of BLM knockdown cells as observed in our laboratory.

Further investigations have revealed that Rmi1 activity is associated with its partners in the BTB complex. First, Rmi1 has directly physical interactions with all three other components of BTB complex. These interactions are essential for this complex's stability. Nevertheless, Rmi1 is also required for normal BLM function. BLM is known to be hyperphosphorylated on Thy-99 and Thy122 in response to mitosis blockage

induced by chemicals or IR, which is ATM-dependent (28, 37). Mutations on either site fail to correct radiosensitivity in BS cell. BLM is also able to translocate to DNA damaged sites or stalled replication forks upon induced genotoxic stress. This translocation is known to be essential for checkpoint activation and damage repair processes. Both activities of BLM are severely impaired in RMI1 depleting cells (82), indicating RMI1 is indispensable for BLM function.

2.4 Introduction of RMI2

Recently, the forth member of BTB complex, Rmi2, has been identified (88, 89). However, its presence in the BTB complex is not evolutionary conserved. In fact, Rmi2 is only expressed in certain vertebrates and plants. Rmi2 directly binds to Rmi1 with its OB-fold Domain but does not have physical interaction with either Topo3 α or BLM. It is required for BTB complex stability. Depletion of Rmi2 protein by siRNA knockdown leads to elevated SCE level, reduced protein level of Topo3 α , Rmi1 and BLM. However, its capacity of maintaining BTB complex stability is depending on Rmi1. Nevertheless, *in vitro* experiments showed that the Rmi1/Rmi2 complex, but not Rmi2 alone could facilitate Topo3 α /BLM resolution activity.

2.5 Activity of BTB complex

2.5.1 RMI1 and Topo3 α are required for BTB complex stability

The structure and function of the BTB complex appear to be evolutionarily conserved among eukaryotes. Physical interactions between Rmi1 and Topo3 α /BLM are required for BTB complex stability (89). Raynard et al. have shown that the N-terminal region of Rmi1 is required for both Topo3 α and BLM interactions (104). Interestingly, Rmi1 and Topo3 α 's stabilities are highly dependent on each other (89). Knockdown of either of them could lead to drastic decreased protein level of the other one. In comparison, BLM protein level is less affected by depletion of either protein, and knockdown of BLM does not diminish Rmi1 and Topo3 α protein levels, as protein levels of both Rmi1 and Topo3 α remain unaffected in BLM knockdown cells.

2.5.2 Biochemical activity of BTB complex

Current model suggests that BTB complex has 'dissolution' activity in processing DSB repair intermediates during the last steps of HR (105). Followed by replication and DNA end rejoining in HR, the invading strand is trapped in between two homologous strands from sister chromatin, and partially annealed to one of them.

This DNA intermediate structure is termed double Holliday junction (DHJ). If not resolved, DHJ could lead to chromosome break during mitosis (106). Several DNA helicases and their complexes are proposed to having activities in resolving this intermediate. All of them are able to physically break and rejoin DNA strand(s). During this process, DNA ends may rejoin to their original strands (non-crossover) or be exchanged to their sister chromatins (crossover). A typical resolving helicase randomly opens nicks on strand(s), which give rise to equal possibilities of both crossover and non-crossover products (107). However, as other candidates may lead to strand exchange between sister chromatins, the BTB complex is specialized in unwinding DHJ using an alternative process termed dissolution, which completely prevents strand exchange between chromatins (79, 103, 108, 109).

Both BLM's DNA helicase and Topo3 α 's DNA Topoisomerase activities are needed during this process. Moreover, these two proteins are non-redundant in DHJ dissolution, as other helicases/Topoisomerases are unable to substitute their functions (103). Although the molecular basis behind this dissolution activity is still poorly understood, a working-model of BTB complex activity has been proposed (107) (**Figure 4.**). Under this model, first, BLM is capable of promoting migration of two HJs together to form another intermediate structure referred as hemicatenine. Next, Topo3 α acts on the hemicatenated DNA substrates to unwind homologous chromatins and complete HR in a non-crossover manner.

Although Rmi1 does not have any known enzyme activity, proper BTB complex activity requires the presence of the Rmi1 protein. The presence of Rmi1 could facilitate HJ unwinding activity of BLM/Topo3 α *in vitro* as the HJ unwinding activity of BLM/Topo3 α combination could be enhanced by as much as 25-fold in the presence of Rmi1 (103). Moreover, under salt conditions mimicking physiological environment, the DHJ dissolution activity of BLM/Topo3 α is completely dependent on Rmi1 presence (110). Interestingly, the Rmi1/Topo3 α interaction is also required for BTB complex activity. The N-terminal fragment of Rmi1 is able to efficiently promote BLM/Topo3 α dissolution activity. Moreover, Rmi1 K166A, a point mutation which ablates its binding with Topo3 α , is unable to promote that activity under the same condition (110). It is very likely that Rmi1 has a regulative role in BTB complex function, where it secures Topo3 α onto DNA substrates.

Nevertheless, the activity of this complex is depended on ATP hydrolysis. The only protein in BTB complex with known ATPase activity is BLM. This suggests that other than its helicase activity, BLM's ATPase activity is also required for this complex's 'dissolution' function (109). In concordance with this, BLM variants with defective ATPase motifs are devoid of HJ unwinding activity.

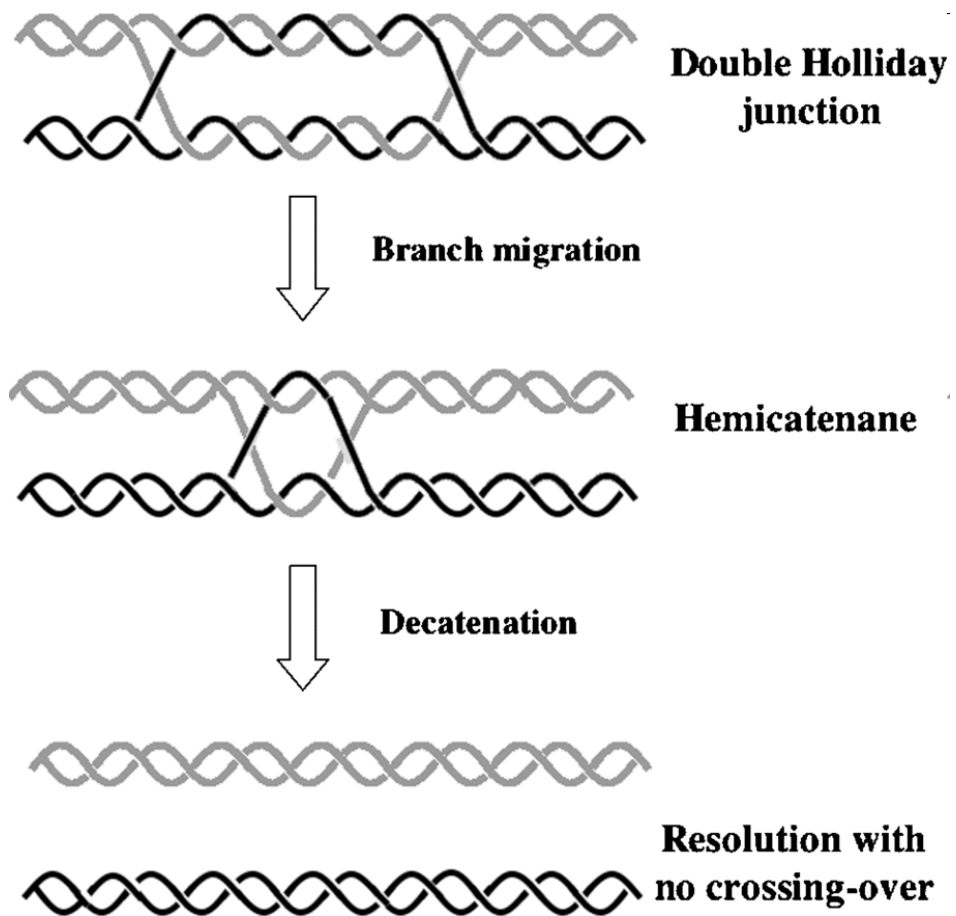


Figure 4. Model of BTB complex 'dissolution' activity. BLM converts DHJ into hemicatenane. This DNA intermediate is the substrate of Topo3 α . This process results in a non-crossover product. Adapted from C.F. Cheok, C.Z. Bachrati, K.L. Chan, C. Ralf, L. Wu and I.D. Hickson, Roles of the Bloom's syndrome helicase in the maintenance of genome stability, *Biochemical Society Transactions* (2005) 33, (1456–1459)

3.0 Mouse models of BTB complex proteins

3.1 Mouse models of BLM

At least three groups have independently generated BLM mouse models. The first two models generated by Chester et al. and Goss et al. both followed similar knockout strategies, from which a part of BLM gene was replaced with a selective marker cassette (23, 111). Both strategies led to lethality of BLM^{-/-} embryo. The BLM^{-/-} model from Chester et al. displayed reduced cell number, increased apoptosis rate and delayed development during early embryonic stages. These embryos eventually die at 13.5 days post coitum (23). The lethality of the other BLM model has not been reported in detail. BLM^{+/-} mice from this group, on the other hand, showed increased cancer susceptibility when injected with murine leukemia virus or crossed with APC mice (111). However, BLM heterozygosity alone does not seem to promote tumor development.

The third BLM mouse model from Alan Bradley's lab was generated by a different strategy, from which the coding sequence of BLM cDNA is disrupted by exon replication (26). Surprisingly, homozygosity of this mutation did not cause embryonic lethality. A possible explanation is that although from its BLM^{-/-} strain, no protein product was detected by anti-BLM antibodies, it is widely believed that unlike the

other two BLM strains with complete absence of BLM gene product, this mutation may retain some of BLM's function. This mouse model partially resembled clinic features of BS syndrome, such as cancer-prone phenotype and elevated SCE level.

3.2 Mouse model of Topo3 α

Topo3 $\alpha^{-/-}$ leads to pre-implantation embryonic lethality. Culturing of Topo3 $\alpha^{-/-}$ blastocysts first showed proliferation defects after hatching, and the growth was completely stopped thereafter (112). Despite the severe phenotype of Topo3 $\alpha^{-/-}$ mice, Topo3 $\alpha^{+/-}$ mice appeared normally.

3.3 Potential application of RMI1 mouse model

We decided to generate a mouse genetic model of RMI1 for the following reasons: First, an animal model of RMI1 could help us better explain the molecular functions of RMI1. Previous advances of RMI1 were mainly accumulated through *in vitro* biochemical assays or experiments conducted in Rmi1 knockdown cell lines. These studies, however, could be influenced by selection of artificial environments or residual effects of remaining Rmi1 protein, respectively. Thus, a complete deletion of RMI1 from the genome at the animal level could provide a bias-free system to study the *in vivo* impact of Rmi1.

Second, RMI1 mouse model may help us to reveal its physiological function. While BLM is known to be associated with BS, Topo3 α and Rmi1 have not been linked to any specific human disorder yet. Thus, the animal models could be one way to study their physiological function. Because of Rmi1's close relationship with BLM, if existing, disorders caused by defective RMI1 in either human or mice could exhibit cancer-prone phenotypes as well. Thus, our RMI1 mouse model could serve as a potential animal model in cancer biology.

Chapter II

RMI1 Is Required for Early Embryonic Development

1.0 Materials and Methods

1.1 Identification and cloning of mRMI1 gene and full-length cDNA

The mRMI1 gene was identified by searching homologous sequence in NCBI database against full-length hRmi1 cDNA. A full-length mRmi1 cDNA clone (BC037694) was obtained from MGC (Mammalian Gene Collection) and used as a probe to screen the RPCI-22 library, a mouse genomic DNA BAC library. To construct this library, DNA extracted from female 129S6/SvEvTac (Taconic) mouse spleen was isolated and partially digested with a combination of EcoRI and EcoRI Methylase before cloning into the pBACe3.6 vector between the EcoRI sites. This

library gridded onto 22x22cm nylon high-density filters for screening was purchased from commercial sources. Three clones hybridized with p³²-labeled mRmi1 cDNA probes, 444B20, 269A5 and 444P22, were identified from my screening. Later, all three BAC clones were shown to contain whole mRmi1 gene sequence. In our study, we used clone 444B20 as the DNA template for vector construction.

1.2 Generation of mouse RMI1 knockout construct

A knockout strategy was designed to replace the only coding exon of mRMI1 (exon 3) with a neomycin selective cassette. A two-step approach was used in generating the knockout construct. First, two DNA fragments located upstream and downstream of RMI1 coding sequence were chosen as recombination targeting arms, respectively. The 4.5kb fragment was referred to as 'long arm', whereas the 1.7kb one was named as the 'short arm', respectively. The two arms were cloned into its own specific vector separately. Second, the two arms with selective markers were rejoined together to form the final knockout construct.

1.2.1 Generating long arm and short arm plasmids

1.2.1.1 Shotgun cloning and identification of long-arm plasmid

Long arm sequence was obtained by direct digestion of the 444B20 BAC DNA with BamHI. Digested BAC DNA fragments were then randomly ligated with pBS-PGK-neo-bpA-LoxB vector. To select colonies carrying the desired fragment, an *in situ* Southern blotting was performed. First, *E. coli* transformed with random ligated plasmid were allowed to grow over night on LB plates and establish colonies. These colonies were transferred onto filter membranes and lysed directly on them by lysis buffer (0.5M NaOH, 1.5M NaCl). Filter membranes were then neutralized by neutralization buffer (1.5M NaCl, 1M Tris, PH=8.0) and washed by 2X SSC before crosslinked to the filter by UV. Next, Southern probe (long arm probe) was amplified by PCR (primers: long arm probe upper: 5'CTTGGCTGTCCTGGAACTCTGT; long arm probe lower: 5'AATGGTTACCCAGGAGCCACTA), labeled with α -p³²-dCTP, and hybridized with filter membranes at 65⁰C overnight. Positive colonies carrying the long arm insert picked. These colonies went on further restrict endonuclease analysis to select the ones with the desirable orientation of cloning.

1.2.1.2 Direct cloning of short arm plasmid

Short arm DNA with embedded PvuII site at its 5' was PCR amplified using BAC DNA as template. The primers are: short arm upper, 5'GTAAAGGGGTGGTGCTGGAATTG; short arm lower, 5'GCATGGCACTAACAACCACAGGA. PCR product was digested by BglII and cloned into pMCI-TK-pA vector.

1.2.2 Construction of final knockout construct

The long arm and adjacent neomycin cassette sequence was released from long arm plasmid by EcoRI/NotI digestion. This fragment was then cloned into the short arm plasmid linearized by SpeI/NotI digestion. The final knockout construct contains two recombination targeting arms, a Cre-floxed neomycin cassette in between two arms and a TK selective marker at 3' of short arm. After recombination, the neo cassette is able to replace entire coding sequence of RMI1, while the TK marker does not integrate into genome.

1.3 Identification of Rmi1 mouse ES cell clones

The construct was transfected into mouse TC1 and G4 ES cells by the Genetically Engineered Mouse Facility (GEMF) at MDACC. Tc1 and G4 ES cells are derived from 100% 129S6/SvEvTac and 50% 129S6/SvEvTac/50% C57BL/6Ner genetic background, respectively. Single ES cells were individually picked into 96-well plates and allowed to form colonies. Then, genomic DNA from each colony were extracted, prepared and hybridized with southern probe for genotyping. Two Southern blot test strategies, which respectively target 5' and 3' DNA sequence of the knockout allele, were utilized in genotyping. The procedures of Southern blot genotypings will be described later in this chapter. In first round of ES cell colony screening, only the 5' strategy was applied. Initially, about 10 colonies from each plate were tested as Rmi1^{+/-} ES cells. These Rmi1^{+/-} colonies were transferred into larger plates, and were subjected to Southern blot tests from both ends again before blastocyst injections.

1.4 Germline transmission

The chimeras were generated by Engineered Mouse Facility (EMF) at MDACC. They were then backcrossed with the C57BL/6 inbred mouse strain for at least 5 generations. Theoretically, genetic material from the original stem cells was reduced to less than 5% thus these experimental mice should be considered as cogenic ones.

1.5 Southern blot tests form ES cell genotyping

Two probes, Probe1 and Probe3, were used in Southern blot genotypings of G-418 resistant ES cell colonies from either 5' or 3' end, respectively. Both probes were amplified by PCR (primers: Probe1A, 5'CCGCCTTTGGTCGTGACTGACAAC; Probe1B, 5'GCTCGGCGGACCTGTTAACACCAG; Probe3A, 5'CTGTGGCTAGAAAGATGGTTCAGC; Probe3B, 5'GAGGGCATGGCCCAGACTTG). For 5' end Southern blot genotyping, genomic DNA of ES cell colonies were directly propagated and digested with NheI overnight in 96-well plates before transferred onto membrane and hybridized with p³² labeled Probe1 overnight at 63°C. For 3' end genotyping, while other conditions remain the same, Probe3 was incubated with PvuII digested genomic DNA and the overnight annealing temperature was 65°C.

1.6 PCR for mice and embryo genotyping

1.6.1 Preparing of Genomic DNA from mice samples

Mice genomic DNA was extracted and purified from mice tissues, usually toes or tail tips. Tissues were first lysed by incubating overnight at 55°C with the mixture of 250

uL lysis buffer (10mM TrisHCl pH8.0, 100mM NaCl, 2.5mM EDTA, 0.5%SDS) and 10uL Proteinase K (20ug/mL). Then, proteins and cell membrane debris were precipitated by 100uL tail salt buffer (4.21M NaCl, 0.63M KCl, 10mMTrisHCl PH8.0) and spinned down at 10,000 rpm for 10 minutes at 4 °C. Genomic DNA then was concentrated by 400uL EtOH and centrifuged at 14,000 rpm for 15 minutes at 4 °C followed by washed with 70% EtOH and dissolved in 200uL ddH₂O.

1.6.2 PCR genotyping strategy of RMI1 mice

For PCR genotyping of RMI1 mice, two pairs of primers were used: LWT3A, 5' CTTTAAGTATCGCCCTCCGTTTTG;
LWT3B, 5'CTTAACATGCCATGTTGCCAAAAG; NS3A, 5' AGCAAGGGGGAGGATTGGGAAGACA; NS3B, 5'GCGGAGCTGCCCCAGCTTTAAGCT. Annealing temperature was set at 61 °C, while the annealing time was 30 seconds for each round.

1.6.3 PCR genotyping strategy of p53 mice

For PCR genotyping of p53 mice, three primers adapted from Genetically Engineered Mouse Facility at MDACC were applied: X6, 5'AGCGTGGTGGTACCTTATGAGC; 7, 5'GGATGGTGGTATACTCAGAGCC;

neo19, 5'GCTATCAGGACATAGCGTTGGC. Annealing temperature was set at 55 °C, while the annealing time was 45 seconds for each round.

1.6.4 Genotyping strategy of RMI1 blastocysts

E3.5 embryos were harvested by flushing uterus with 1X PBS. A nested PCR strategy was applied for genotyping. Two pairs of primers were used in first round of PCR: LWT1A, 5'CTCATCCCAGAGTAAGGTGGCCGACTAT; LWT1B, 5'CACAAGCTTCCAGCCACATTGGAGGTAC; NS2A, 5'TTCGCAGCGCATCGCCTTCTATCG; NS2B, 5'AGCAGGGTCTCGCCTTTTGCCTCGAGAG. The primer pairs, LWT3 and NS3 were used in the following second round PCR.

1.7 Cell culture and Clonogenic survival assay

Cell strains were maintained in 10% heat-inactivated fetal bovine serum and grown in a humidified 5% carbon dioxide (CO₂)-containing atmosphere at 37°C.

Procedures of Rmi1 siRNA knockdown and Clonogenic assay were applied as described previously (82). Briefly, HCT116 cells were transiently transfected with either Rmi1 or control (luciferase) shRNA before counted and seeded onto 100mm plates. Colonies were allowed to grow for 2 weeks before counting.

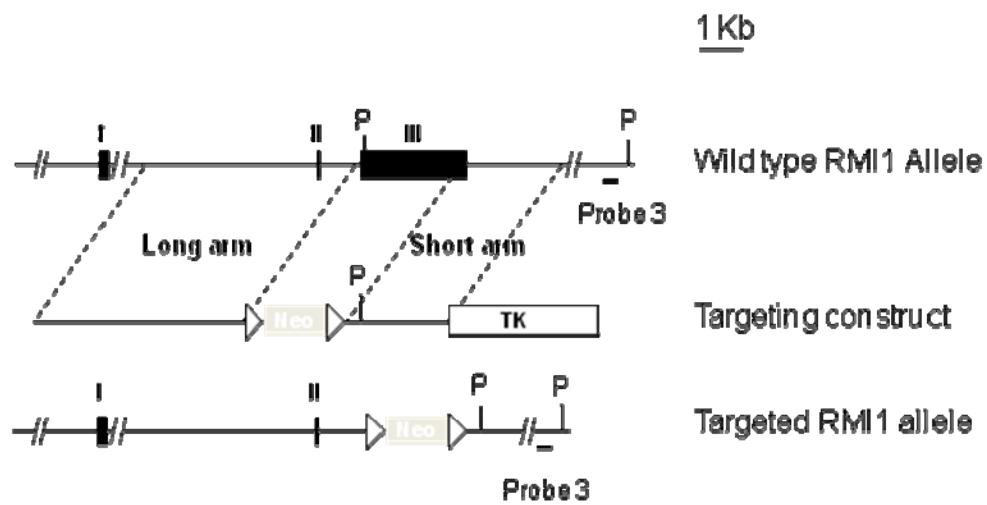
2.0 Results

2.1 Generation of RMI1 knockout mouse model

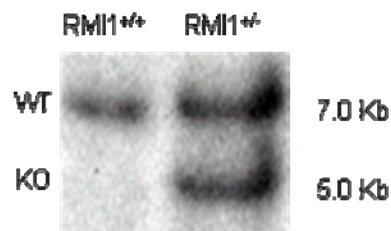
We generated a RMI1 knockout mouse strain by replacing its exon 3, which contains the entire RMI1 coding sequence of 1.8 kb, with a Cre-floxed neomycin selective cassette. This replacement created a null-allele of RMI1 (**Figure 5A.**).

ES cells carrying one copy of the targeted allele were selected through several rounds of Southern blot genotypings, using probes locating on either 5' or 3' of the long and short arms, respectively (**Figure 5B.**). Screening of a total of 192 ES cell clones showed that my general targeting frequency is 12%. RMI1^{+/-} clones identified by both 5' and 3' probes were used to generate chimeras through standard blastocyst injection. After successful germline transmission, RMI1^{+/-} founders were genotyped by PCR and backcrossed to C57BL/6 background for at least 5 generations (**Figure 5C.**).

A



B



C

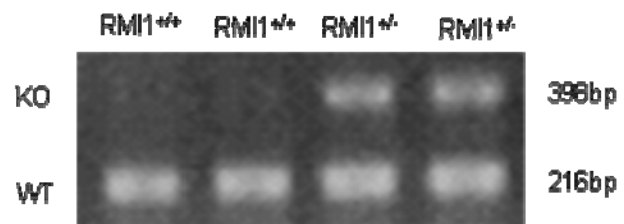


Figure 5. Replacement targeting of the RIM1 locus. **A.** Strategy of RIM1 replacement targeting. P: PvuII sites for Southern Blot genotyping. Solid boxes depict the three RIM1 exons (I, II, and III). Neo: Neomycin selection marker (positive marker). Open triangles: CreLoxP sites. TK: TK cassette (negative selection marker). **B.** Southern blot of Pvu II-digested genomic DNA from RIM1^{+/+} and RIM1^{-/-} ES cells with the 3' probe. WT: wild type allele. KO: Targeted allele. **C.** typical PCR genotyping results of RIM1^{+/+} and RIM1^{-/-} mice using genomic DNA extracted from tail clips. Adopted from Haoyi Chen, et.al., RIM1 Attenuates Tumor Development and is Essential for Early Embryonic Development (accepted by Molecular Carcinogenesis).

2.2 Embryonic lethality of RMI1^{-/-} mice

A small group of RMI1^{+/-} mice was put on long-term observation for up to 3 years.

These mice do not display any noticeable defects in fertility, life span and spontaneous tumor onset. However, intercross of Rmi1^{+/-} mice did not produce any mice with RMI1^{-/-} genotype, indicating an Rmi1-dependent embryonic lethality.

To determine the time of embryonic lethality, I dissected pregnant females after RMI1^{+/-} mice intercrossing. First, attempts to recover RMI1^{-/-} MEF cells from 13.5 dpc embryos failed, as only wild type and RMI1^{+/-}, but not RMI1^{-/-} MEF cells were collected from all MEF cells established. Subsequently, more females were dissected at different stages of pregnancy. However, no RMI1^{-/-} embryos were identified as early as 7.5 dpc. To further investigate this question, I performed blastocyst analysis. At day 3.5 dpc, neither abnormal nor RMI1^{-/-} blastocysts were identified from RMI1^{+/-} crossing (**Table 1**).

At the same time, the wild type and RMI1^{+/-} embryos recovered from both embryo dissection and blastocyst flushing displayed a nearly perfect 1:2 ratio, which strictly

Date	+/+	+/-	-/-
E3.5	7	11	0
E8.5	11	18	0
E9.5	6	12	0
E10.5	2	6	0
Summary	19	36	0

Table 1. Summary of embryonic genotypes. Embryos were harvested between 3.5 to 10.5 dpc from RMI1^{+/+} intercrossing. Adopted from Haoyi Chen, et.al., RMI1 Attenuates Tumor Development and is Essential for Early Embryonic Development (accepted by Molecular Carcinogenesis).

followed the Mendelian segregation. From these results, I concluded that RMI1 is required for early embryonic development, and deleting both alleles of RMI1 leads to embryonic lethality before implantation.

2.3 p53-dependent cell proliferation in Rmi1-depleted cells

We next investigated the mechanism of Rmi1-dependent embryonic lethality. Knockdown Rmi1 in tissue culture cells destabilized the BTB complex and enhanced the SCE level. Nevertheless, cells transfected with shRNA vectors were unable to form colonies. We suspect that the increased genomic instability from lack of Rmi1 might be the primary cause of cell lethality.

To address this hypothesis, I performed the clonogenic survival assay. I transfected Rmi1 shRNA as well as control RNA (luciferase) into both HCT116 and its isogenic p53-null strains. Clonogenic survival assays were conducted after transient transfection and G418 selection. In accordance to our previous data (81), knockdown Rmi1 resulted in drastic decrease in colony survival rate. p53-null background per se had little effect on colony formation when transfected with the control luciferase shRNA construct. Interestingly, absence of p53 in Rmi1 depleted cells significantly rescued its colony formation ability, as colony survival increased by 10-fold when comparing with that from Rmi1-depleting cells alone (**Figure 6A, B.**). This data strongly argues for a potential functional relationship of RMI1 and p53 in

regulating cell viability. Most likely, lack of p53 allows cells to continue to proliferate when genomic lesions are accumulated as a result of Rmi1 loss.

2.4 p53^{-/-} did not alleviate early embryonic lethality of RMI1^{-/-} mice

Since p53^{-/-} background effectively mitigated the cellular lethality of Rmi1 knockdown cells, it is likely that deletion of p53 alleles may extend RMI1^{-/-} embryos' life span to beyond the implantation stage. This observation would suggest that loss of RMI1 leads to genomic stresses that are dealt with by the p53-dependent pathways. To address this possibility, I performed embryonic analysis on D3.5 blastocysts collected from p53^{+/-}RMI1^{+/-} intercrossing. Of all 47 blastocysts collected, 17 were RMI1^{+/+} and 28 were RMI1^{+/-}. None of them, however, was RMI1^{-/-}. This result indicates that deleting either one or both alleles of p53 is unlikely to extend viability of RMI1^{-/-} embryos passing the implantation stage. (P<0.05), suggesting a high degree of severity resulting from RMI1 deletion.

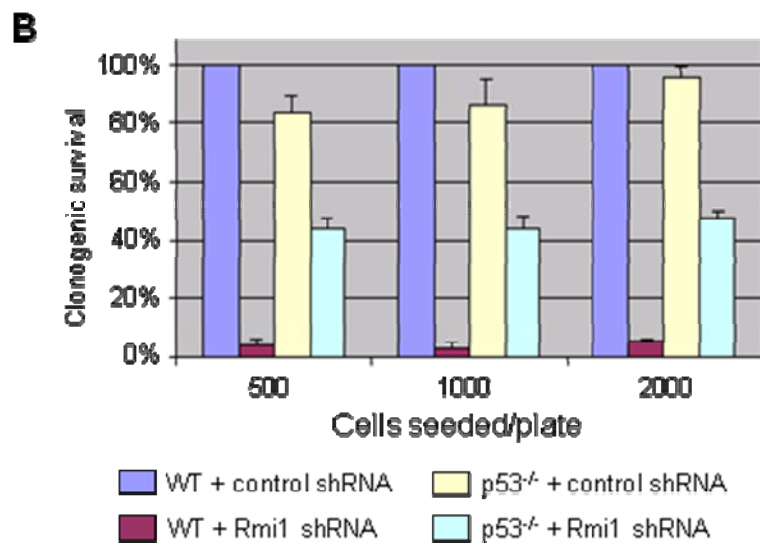
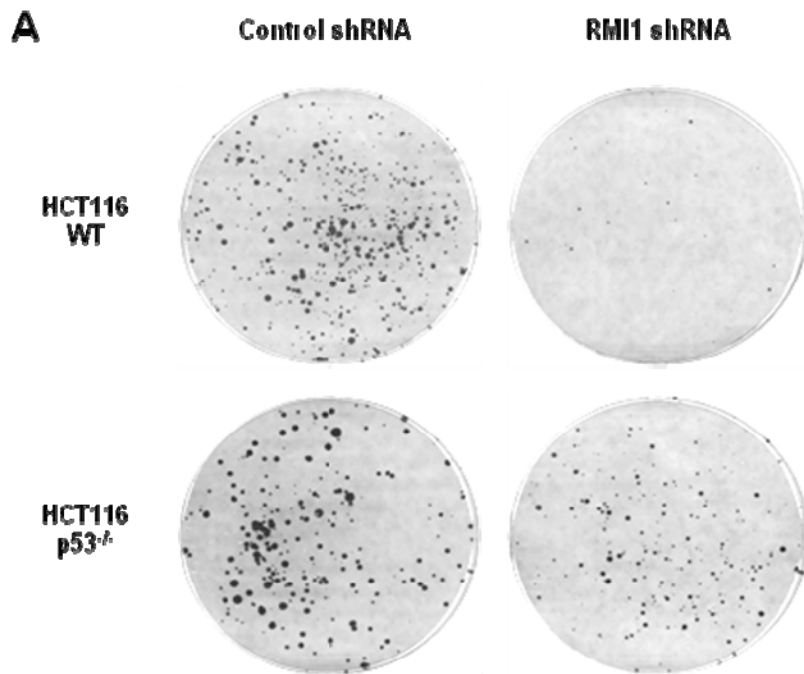


Figure 6. Clonogenic survival assay of Rmi1 knockdown in HCT116 cells. Rmi1 shRNA and control RNA (Luciferase) were transfected into both p53^{-/-} HCT116 cell and its isogenic strain, respectively. a. Typical plates from clonogenic survival assay. b. Colony numbers from each group were counted and normalized against data collected from HCT116 transfected with control RNA. Adopted from Haoyi Chen, et.al., RMI1 Attenuates Tumor Development and is Essential for Early Embryonic Development (accepted by Molecular Carcinogenesis).

3.0 Discussion

3.1 RMI1 is essential for early embryonic development

The RMI1 knockout mouse model allowed us to investigate its function in embryonic development. Our data demonstrated that RMI1 is required for embryo viability.

Complete deletion of this gene led to early lethality before implantation stage.

Our finding, together with previous studies, shows that all three conserved components of BTB complex, including BLM, Topo3 α and RMI1, are required for embryonic development. However, their phenotypes of lethality are distinct. BLM^{-/-} embryos die at 13.5 dpc whereas Topo3 α ^{-/-} embryos die before implantation stage. In our study, we've demonstrated that similar to Topo3^{-/-} ones, RMI1^{-/-} embryos die at the same, if not earlier, embryonic stage.

The mechanism that leads to RMI1-dependent lethality remains unknown. To our best knowledge, until recently, no catalytic activity had been identified for Rmi1. It is very likely that Rmi1 performs a non-catalytic, regulative function in the BTB complex. Thus, the lethality of RMI1^{-/-} embryos could be contributed to relationship between RMI1 and BLM/Topo3 α . Physical presence of Rmi1 is required for BLM-Topo3 α complex stability and activity, which has been evidenced by Rmi1 knockdown experiments. Based on that, it is reasonable to believe that complete absence of Rmi1 could further diminish stability of BLM and Topo3 α proteins,

possibly under threshold of maintaining their proper cellular functions. The lethality of RMI1^{-/-} embryos, under this scenario, is the compounded consequences of both functional and physical deficits of BLM and Topo3α.

It is notable that in comparing with BLM, Topo3α might play a major role in RMI1-dependent embryonic lethality. This view is supported by previous experiments. First, Topo3α protein levels could be more significantly affected by RMI1 knockout. Previous studies from our and Dr. Weidong Wang's lab suggest that depleting Rmi1 results in moderate and drastic decrease of protein level of BLM and Topo3α, respectively, which indicates that the Topo3α protein is more likely be reduced to insufficient levels than BLM. Secondly, defective BLM function alone does not explain early lethality of RMI1^{-/-} embryos. BLM^{-/-} embryos show retarded growth and die at 13.5 dpc. Thus, the absence of BLM protein alone may not be the cause of this pre-implantation lethality. On the other hand, the lethal phenotype of Topo3α^{-/-} embryos is reminiscent of that of RMI1 mice. This similarity of phenotypes could indicate a functional relationship of RMI1 and Topo3α.

RMI1^{-/-} embryos could die from mitotic dysfunction. Rmi1 is found in two independent complexes. One is the BTB complex. The other one contains only Rmi1/2 and Topo3α without BLM. This indicates that Rmi1 and Topo3α together may have cellular function other than 'resolution' in HR. Nevertheless, yeast top3 mutations exhibited sporulation and chromosome separation defects during mitosis. Moreover, knockdown Topo3α in mammalian cells led to abnormal anaphase bridge

formations. It is plausible that RMI1 deletion leads to defective mitotic function due to insufficient protein level of Topo3 α , and eventually, cell death.

However, it is still unclear whether RMI1 itself has any direct role in maintaining embryo viability. Although Topo3 $\alpha^{-/-}$ embryos also die before implantation, normal deciduae (Topo3 $\alpha^{+/-}$ and wildtype) as well as smaller ones contained no organized embryos were dissected from Topo3 $\alpha^{+/-}$ intercrossing. On the other hand, we have not found any of such deciduae from RMI1 $^{+/-}$ intercrossing, suggesting a possible earlier lethality of RMI1 $^{-/-}$ embryos in comparison with Topo3 $\alpha^{-/-}$ ones. The earlier lethality of RMI1 $^{-/-}$ embryos could be caused by compounded outcome of defective activities from both BLM and Topo3 α . It is also possible that besides its regulative role with BLM and Topo3 α , RMI1 yields unknown function in maintaining cellular viability.

3.2 Functional relationship of Rmi1 and p53

p53 is one of the most active regulators in DNA damage-induced cell cycle arrest and apoptosis pathways. The protein-protein interaction between p53 and BLM has been revealed, whereas an N-terminal region of BLM is mapped as respective interaction segment for p53 binding. P53 may regulate BLM function during homologous recombination (HR) pathway, where it could interact with DNA recombination intermediates and prohibit helicase activity of BLM. Interestingly, p53

is dependent for DNA damage-induced apoptosis in BS cells. Additional deleting of p53 rescues cell death of BS cells followed UV or MMC treatments. Because of the close relationship between BLM and Rmi1, p53 may also play a significant role in RMI1-associated cellular viability.

In our experiment, we have demonstrated that p53-null alleviates cellular lethality of Rmi1 depleting cells. However, deleting p53 alleles in RMI1^{-/-}embryos did not extend their viability beyond the implantation stage. A plausible explanation is that the genomic integrity is more strictly required during embryonic development. These results strongly argue for our hypothesis that Rmi1 depleting cells die from compromised genomic integrity.

Chapter III

RMI1 Heterozygosity Accelerates Induced-tumor Formation of p53^{+/-} Mice

1.0 Materials and Methods

1.1 Ionizing radiation treatment and tumor analysis of animal model

Littermates from Rmi1^{+/-}-p53^{+/-} intercrossing were subjected for IR irradiation at 4GY (NASATron) around 6 weeks of age. A daily observation was applied to all irradiated mice for at least 1 year or until death. Those with visible tumor phenotypes were sacrificed and sent for necropsy. Tissue samples were preserved

in 10% formalin. For histopathological analysis, samples were embedded in paraffin cassettes prior to slide cutting and staining by hematoxylin&eosin (H&E). Kaplan-Meier methods was applied to estimate survival rate. Survival curves and P value calculation were carried by software GraphPad Prism.

1.2 Extraction of genomic DNA from fixed specimens

Pieces of mouse tissue samples fixed by 10% formalin were first washed by running water overnight, then, chopped into fine pieces by scissors in 1.5ML tubes. Next, as previously described, standard genomic DNA extraction protocol was applied. Genomic DNA was dissolved in 50uL ddH₂O.

1.3 Preparation MEF cells

Females were euthanized at day 13.5. The ovaries were transferred into 10cm tissue culture dishes and washed with 1X PBS containing 2X pen/strep under sterilized environment. Each embryo was transferred into a new dish, removed from all mother tissue, and minced well with a surge knife. The embryo was then incubated with 1 ml 0.25% Trypsin/EDTA at 37 °C for 10 minutes, added with 10 ml DMEM with 10% FBS, mixed by gently pipetting the medium 10 times and placed at 37 °C with 5% CO₂ for 24 hours. The MEF cells were spited or frozen when confluent.

1.4 Immuno-staining of radiation-induced foci

MEF cells were allowed to grow on cover slips and irradiated at 1.5Gy at desired time points. The cover slips were washed once with 1X PBS, fixed by 1ml 3% Paraformaldehyde for 10 minutes at RT. The slips then were washed once with 1XPBS, treated with 1ml 0.5%Triton buffer for 5 minutes at RT, and washed twice with 1X PBS. The primary antibodies, diluted in 1:1000 ratio with 5% Goat Serum, were applied directly at the center of slips and the slips were incubated overnight at 4 °C. The secondary antibody, diluted in 1:2000 ratio with 5% Goat Serum, were applied and incubated for 20 minutes at 37 °C. All the antibodies are kindly gifts from Dr. Junjue Chen of MDACC. A drop of Mounting medium was applied to each slip before it was fix to a slide by sealing all edges with nail varnish.

2.0 Results

2.1 Shortened half-life of radiation-induced foci in p53^{+/-}RMI1^{+/-} MEFs

The BTB complex is known to maintain genomic integrity through the HR pathway during DSB repair. The impact of RMI1 deficiency on genomic integrity may further be facilitated under a p53^{+/-} background. Therefore, I tested the radiation-induced foci status in p53^{+/-}RMI1^{+/-} MEFs. The control MEFs, consisted of wild type, p53^{+/-}, and RMI1^{+/-} genotypes, were derived from littermates of p53^{+/-}RMI1^{+/-} intercrossing. To do so, I obtained intercross between p53^{+/-}RMI1^{+/-} males and females and harvested embryos at [D13.5](#). Four MEF cell lines were generated from littermates with the following genotypes, p53^{+/+}RMI1^{+/+}, p53^{+/-}RMI1^{+/-}, p53^{+/+}RMI1^{+/-}, and p53^{+/-}RMI1^{+/+}.

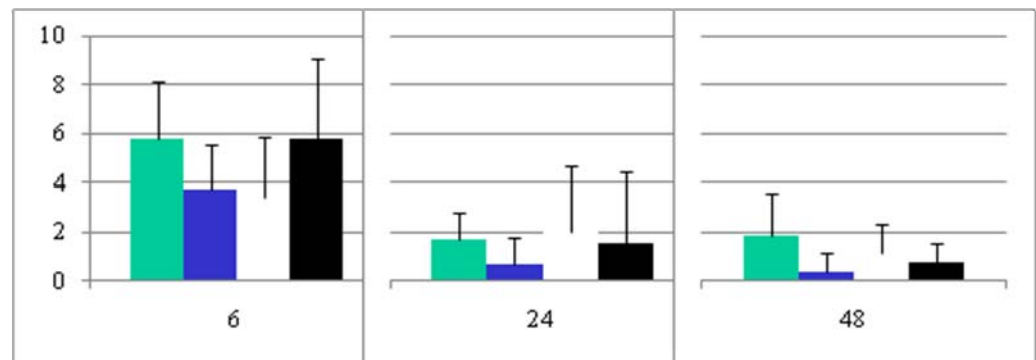
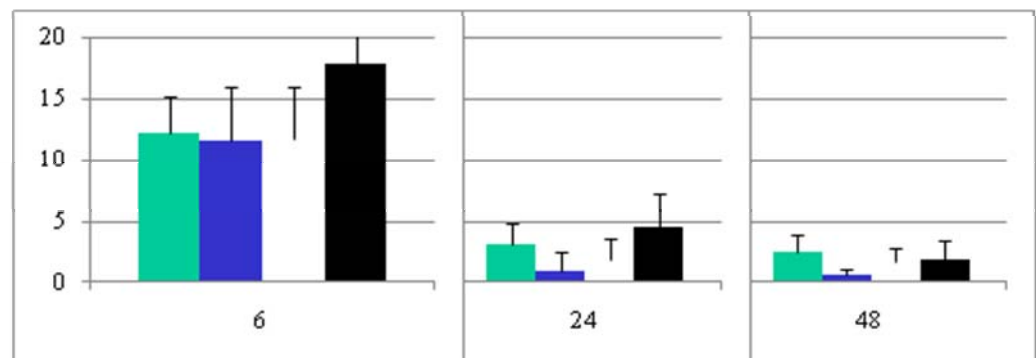
All the MEFs were subject to 1.5Gy of ionizing radiation. The nuclear focus formation was stained by either γ -H2AX or 53BP1 antibody and scored at various time points up to 48 hours after radiation. Initially, the numbers of foci observed per cell were similar among p53^{+/-}RMI1^{+/-} and control MEFs. (**Figure 7.**) However, after 24 or 48 hours, the average number of foci per p53^{+/-}RMI1^{+/-} MEF nucleus is moderately lower than any of the control MEFs.

It is more noticeable that at 24 or 48 hours post IR, a substantial proportion of cells had already lost detectable foci and became foci-negative. This phenomenon was observed from MEFs of all genotypes. However, when comparing with control MEFs,

p53^{+/-}RMI1^{+/-} MEFs had a significantly higher percentage of foci-negative population. (**Table 2.**) While the foci-negative p53^{+/-}RMI1^{+/-} MEFs constituted more than 60% of the total population, the percentages of foci-negative control MEFs were between 25~45%. This result suggests an accelerated resolution of radiation-induced foci in p53^{+/-}RMI1^{+/-} MEFs, presumably due to the partial loss of RMI1, which allows Holliday junctions to be resolved without the deterrence of the BTB complex function and in conjunction with the deficient p53 status.

2.2 Ionizing radiation fails to induce enhanced tumor formation in RMI1^{+/-} mice

The BTB complex proteins are known for their function in maintaining genomic integrity partly by preventing chromatid exchanges during HR. Because of its role in this complex, it is very likely that loss of one RMI1 allele could affect the overall level of the BTB complex activity. This disruption might impact the efficiency or/and outcome of DSB repair, because elevated recombination events may cause LOH in tumor suppressor gene alleles, and consequently, lead to increased tumorigenesis. Moreover, as indicated by my results at the cellular level, p53 deletion effectively mitigated the cell lethality caused by Rmi1 depletion. Thus, it is possible that compromised p53 function may facilitate or enhance any potential haploinsufficiency of the Rmi1 gene. Following this idea, I constructed RMI1 and p53 double heterozygous mouse model. I exposed RMI1^{+/-} as well as wild type, RMI1^{+/-}p53^{+/-} and p53^{+/-} mice to sub lethal dosage of IR. Four groups of mice were treated with 4Gy of gamma radiation at an age of 6 weeks. These mice were then kept for

A**B**

■ Rmil +/- p53+/+
■ Rmil +/- p53+/-
■ Rmil +/- p53+/-
■ Rmil +/- p53+/+

Figure 7. Foci Staining 6, 24, and 48h after IR (1.5Gy). **A.** 53BP1 staining. **B.** Gamma-H2AX staining.

	Hours after IR	Rmi1 ^{+/-}	Rmi1 ^{+/-} p53 ^{+/-}	p53 ^{+/-}	Wild type
53BP1	24h	27.8±3.2%	66.4±12.5%	41.6±7.5%	48.8±4.3%
	48h	28.4±5.0%	80.6±7.0%	56.7±4.3%	45.8±10.6%
H2AX	24h	24.6±5.4%	61.7±9.1%	35.6±11.3%	15.3±23.2%
	48h	28.3±2.4%	60.4±6.4%	38.5±8.7%	29.5±6.1%

Table 2. Summary of foci-negative MEF populations 24 or 48 hours after IR (1.5Gy). Adopted and modified from Haoyi Chen, et.al., RMI1 Attenuates Tumor Development and is Essential for Early Embryonic Development (accepted by Molecular Carcinogenesis).

observation of tumor formation for at least a year. All the mice were euthanized at the end of the tumor monitoring. As shown in **Table 3**, although more mice developed tumor before 35 weeks of age, the overall tumorigenesis rate of RMI1^{+/-} mice (23%, 5/22) is indistinguishable from that of wild type controls (31%, 8/26). Thus, RMI1 heterozygosity alone seems unable to cause increased tumorigenesis, both spontaneous and induced.

2.3 Rmi1 heterozygosity accelerates IR-induced tumor formation of p53^{+/-} mice

Expectedly, the majority of p53^{+/-} mice developed tumors (75%, 15/20). Interestingly, although overall tumorigenesis rate of RMI1^{+/-}p53^{+/-} (83%, 19/23) mice is close to that of the p53^{+/-} mice, more mice from this group developed tumors at earlier ages than p53^{+/-} ones. The tumor incidence is 52% (12/23) by 35 weeks of age, and 74% (17/23) by 55 weeks of age, respectively. In comparison, percentages from p53^{+/-} group are 10% (2/20) and 50% (10/20) by the same time points, respectively. Moreover, the average tumor free rate is 27 weeks from RMI1^{+/-}p53^{+/-} mice, comparing with 45 weeks from p53^{+/-} ones. The difference of average tumor free rate from two groups is statistically significant ($P < 0.02$) (**Figure 8.**). Clearly, our result indicates a relationship between p53 and RMI1 in accelerated tumorigenesis.

Previous studies have shown that irradiated p53^{+/-} mice develop lymphoma as primary tumor. Depending on the background of the inbred strains, 48% to 90% induced tumors from p53^{+/-} mice are lymphoma. In our experiment, a similar trend

was observed. Lymphoma consisted the primary source of identified tumors derived from p53^{+/-} mice.

	No. of mice	No. of mice died	No. of mice died within 35 wks	lymphoma	sarcoma	sarcoma	unknown
Rmi1 ^{+/-} p53 ^{+/-}	23	29	12	12	5	4	1
Rmi1 ^{+/+} p53 ^{+/-}	20	25	2	7	3	3	5
Rmi1 ^{+/-} p53 ^{+/+}	22	7	3	3	2	0	2
Rmi1 ^{+/+} p53 ^{+/+}	26	9	1	8	2	0	1

Table 3. Summary of induced-tumors from Rmi1^{+/-} p53^{+/-} and control groups.

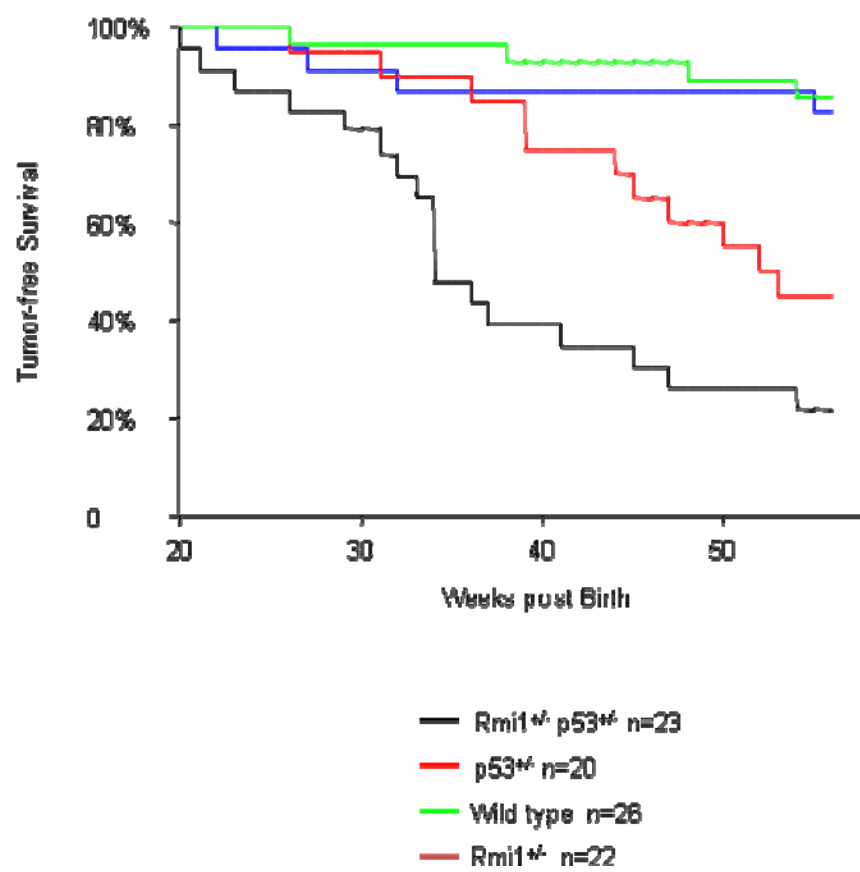


Figure 8. Accelerated and enhanced IR-induced tumorigenesis in Rmi1^{+/+} p53^{+/+} mice. Rmi1^{+/+} p53^{+/+} mice, and control groups (p53^{+/+}, Rmi1^{+/+}, and wild type) were exposed to 4 Gy of ionizing radiation at the age of 4 weeks. Tumor-free survival was monitored for 1 year after irradiation. Adopted from Haoyi Chen, et.al., RMI1 Attenuates Tumor Development and is Essential for Early Embryonic Development (accepted by Molecular Carcinogenesis).

(47%, 7/15), more than carcinoma and sarcoma combined. On the other hand, RMI1^{+/-}p53^{+/-} mice developed higher percentage of lymphoma (57%, 12/23) (**Table 3.**). However, it requires further study to determine whether the difference of lymphoma occurrences from the two groups is statistically significant. Together, the additional deletion of RMI1 does not seem to alter the overall tumor spectrum of the p53^{+/-} mice.

Interestingly, in comparison with p53^{+/-}, RMI1^{+/-}p53^{+/-} mice exhibited higher risk to aggressive tumor types, which include high grade lymphoma, invasive carcinoma, and invasive osteosarcoma as illustrated in **Figure 9A-F**. In summary, deleting one copy of RMI1 gene under p53^{+/-} background leads to accelerated tumor onset and potentially more aggressive tumor types, both of which indicate a tumor suppressor role of RMI1.

2.4 LOH assays on RMI1 and p53 loci

Loss of heterozygosity (LOH) of p53 locus occurs frequently in p53^{+/-} tumors. It is very likely that LOH on RMI1 locus may cause accelerated tumor formation in RMI1^{+/-}p53^{+/-} mice. In this project, I tested this hypothesis by studying LOH on both loci. Genomic DNA from tumor tissue and tail tips of RMI1^{+/-}p53^{+/-} mice are collected and PCR genotyping was performed. Interestingly, whereas tumor cells lost wild type p53 alleles, the heterozygosity of RMI1 locus sustained (**Figure 10A.**). Thus,

LOH of RMI1 locus seems not the cause of tumor-formation phenotype observed in RMI^{1+/-}p53^{+/-} mice. However, because genomic DNA extracted from fixed tumor specimens were unable to produce clear PCR results (**Figure 10B.**), probably due to fragmentized genomic DNA, more data is needed in order to firmly establish this hypothesis.

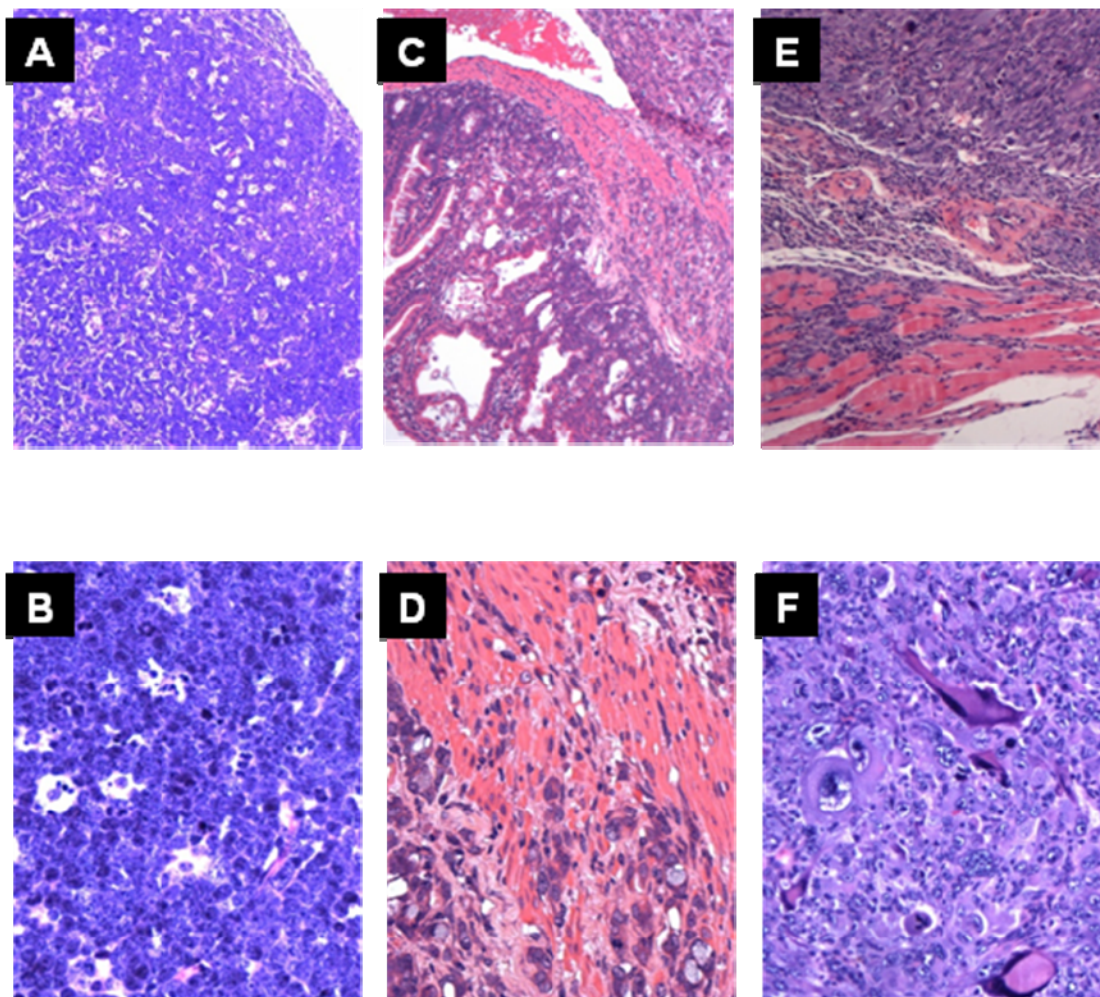


Figure 9. Aggressive tumors derived from the RMI1^{+/-} p53^{+/-} mice, H & E stains. A and B, High grade lymphoma involving a lymph node (A, 100×; B, 400×). C and D, Aggressive and invasive adenocarcinoma of small intestine (C, 100×; D, 400×). E and F, Aggressive and invasive osteosarcoma involving skeletal muscle (E, 100×; F, 400×). Adopted from Haoyi Chen, et.al., RMI1 Attenuates Tumor Development and is Essential for Early Embryonic Development (accepted by Molecular Carcinogenesis).

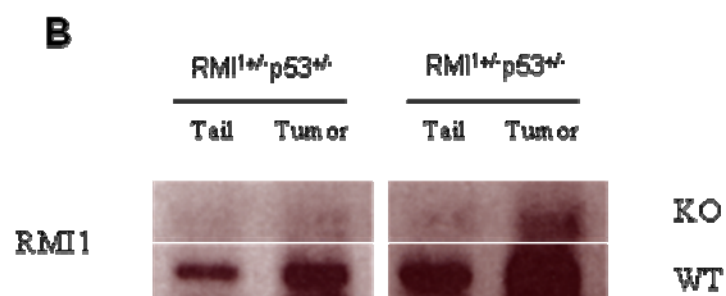
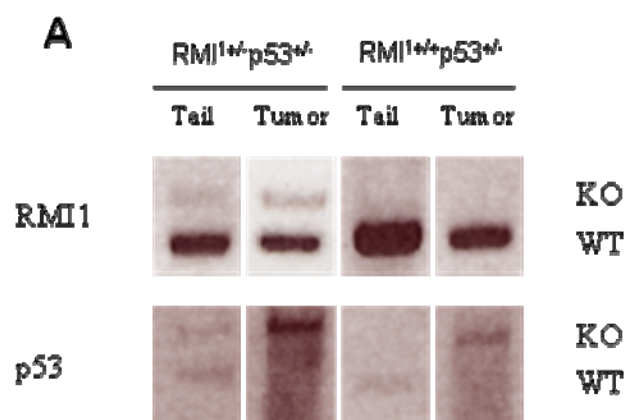


Figure 10. LOH assay of RMI1 and p53 loci. **A.** Genotyping of RMI1 and p53, using genomic DNA extracted from tail and tumor tissues, respectively. **B.** LOH assay of RMI1 locus, genomic DNA was extracted from 10% formalin fixed specimens.

3.0 Discussion

3.1 Functional relationship between p53 and RMI1

I have shown that radiation-induced foci were more rapidly resolved in RMI1^{+/-} p53^{+/-} MEFs, when compared to MEFs derived from wild type, RMI1^{+/-} p53^{+/+}, and RMI1^{+/+} p53^{+/-} embryos. This accelerated resolving rate is unlikely caused by cell death, since no significant difference was found among MEF cells with the four different genotypes when assayed for radiation-induced apoptosis with the same dose of radiation.

While p53-deletion mitigated cell death of RMI1-depleted cells, p53^{-/-} background fails to extend the viability of RMI1^{-/-} embryos to blastocyst stage. In the foci experiment, however, p53 and RMI1 double heterozygous MEFs displayed a measurable phenotype compared to control MEF cells, indicating a functional interaction between p53 and RMI1. These results reflect the abilities of different experimental systems when genetic interactions are investigated. It also suggests that the requirement for RMI1 and p53 functions is not identical among transformed cell, MEF cells, and mouse embryos. However, the commonality in the observed phenotypes is consistent with the notion that the BTB complex acts to facilitate non-crossover HR repair and prevent excessive or nonreciprocal exchanges. Thus, RMI1 deficiency in general will lead to genomic instability of varying extent. A p53 deficient

background likely substantiates the defects by suppressing checkpoint mechanisms. However, the exact role of p53 in association with RMI1 remains unknown.

3.2 Recessive haploinsufficiency of RMI1^{+/-} mice

RMI1^{+/-} mice are viable and productive. At the same time, deleting one copy of RMI1 allele does not lead to either spontaneous or radiation induced-tumor formations. Challenged by IR of 4 Gy at 6 weeks of age, 3 RMI1^{+/-} mice died within 35 weeks. By the end of the experiment, 7 deaths were observed out of 22 individuals. In comparison, these numbers are 1 and 9 out of 26 in wild type control cohort, respectively. The tumor-free survival curves from two cohorts are not significant different within either 35 or 55 weeks of period. RMI1 heterozygosity does not alter the tumor spectrum, too. Both mice mainly developed lymphoma and sarcoma. Although the percentage of lymphoma incidences from RMI1^{+/-} mice was much lower than that from wild type ones, it could be simply due to insufficient sample size.

These results are consistent with phenotypes observed from both BLM and Topo3 α heterozygous mice. However, haploinsufficiency has been observed in BLM mice. BLM^{+/-} mice die earlier when injected with murine leukemia virus (MLV). Furthermore, the BLM/APC double-heterozygous mice exhibited enhanced gastrointestinal tumor formation. Thus it is very likely that RMI1 mice could display similar haploinsufficient cancer-prone phenotypes under certain condition.

We approached RMI1 function in tumorigenesis by crossing RMI1^{+/-} mice with p53^{+/-} ones. Interestingly, the RMI1/p53 double heterozygous mice, unlike RMI1^{+/-} and p53^{+/-} ones, exhibited accelerated radiation induced-tumor formation. At the age of 35 weeks, 12 out of 23 RMI1^{+/-} p53^{+/-} mice had died, whereas only 3 out of 22 and 2 out of 20 mice died from RMI1^{+/-} and p53^{+/-} groups, respectively. This early tumor onset indicates a recessive haploinsufficiency of RMI1 function in tumor susceptibility.

Despite accelerated tumor onset, RMI1^{+/-}p53^{+/-} mice did not display altered tumor spectrum from p53^{+/-} mice. p53^{+/-} mice received sub-lethal dosage of IR are known to be prone to a wide spectrum of tumors. Although the profiles of tumor spectrum might vary depending on strains and radiation dosage, lymphoma is the primary source of tumor types. In our study, about half of IR induced-tumors from p53^{+/-} and RMI1^{+/-}p53^{+/-} mice consisted of lymphoma. Moreover, both mice developed sarcoma and carcinoma.

It is notable that RMI1^{+/-}p53^{+/-} mice had increased risk to aggressive tumor types. In our limited study, we have observed high-grade lymphoma, invasive carcinoma and invasive osteocarcinoma. In contrast, few mice from p53^{+/-} as well as other two groups developed such high-grade tumors. It is thus very likely that in addition to accelerating tumor onset, RMI1 heterozygosity, in combination with p53^{+/-}, might

facilitate the progression of malignancies, too. However, in order to firmly establish this point, further study involved larger sample pool may be required.

The mechanism between RMI1 heterozygosity and earlier tumor onset of p53^{+/-} mice remains elusive. LOH of p53 locus is a common phenotype of p53^{+/-} tumors. Our preliminary study of LOH in RMI1^{+/-}p53^{+/-} tumor samples suggested that while the wild type p53 allele was lost, the wild type RMI1 allele, on the other hand, was not. BS cells are known for its elevated gene targeting/recombination efficiency, indicating BLM, as well as BTB complex function in maintaining genomic stability and integrity. It is very likely that RMI1 heterozygosity reduces BTB complex activity, and leads to promoted genomic recombination events. Thus in RMI1^{+/-} cells, although the cellular viability and DNA damage checkpoint/repair pathways may remain intact, LOH on p53 locus could be facilitated by this RMI1-associated enhanced recombination efficiency. This results in accelerated tumor onset.

In summary, we argue for a potential tumor suppressor role of RMI1. Although deleting one copy of RMI1 gene did not lead to increased risk of both spontaneous and induced tumor formation in animal model, it facilitated tumor onset when coupled with p53 heterozygosity.

3.2 Potential clinic application of RMI1 mouse model

Until recently, RMI1 gene has not been linked to any specific genetic disorders. Our experiment, however, demonstrated that RMI1^{+/-} in combination with p53^{+/-}, contributes to significant accelerated radiation-induced tumorigenesis. This result suggests RMI1 heterozygosity, when coupled with defective tumor suppressor genes, could lead to higher risk, earlier onset and poorer outcome of tumors. Thus, because its haploinsufficient impact on tumor susceptibility, RMI1 should be considered as an tumor suppressor gene.

Recently, the clinical outcome of single nucleotide polymorphisms (SNPs) has been studied extensively. By definition, polymorphism is the least common allele occurring in 1% or greater of the population (113). SNPs are present throughout human genome. The average frequency of SNPs is approximate 1 per 1,000 base pairs (bp) (114). It is well established that certain SNPs are associated with cancer susceptibility. Depending on the context of the SNP, it could be either protective or provocative in cancer risk (115, 116).

Several SNPs from RMI1 gene have been linked with increase risk of cancers in clinical studies. In predominating Swedish population, SNP (rs1982151) carriers have about 2-fold and 1.5-fold higher risk of AML/MDS and MN than controls, respectively. This association between risk of cancers and RMI1 SNP is observed both in heterozygotes and homozygotes. Moreover, the effect of age was found

during this study, especially in MN patients (117). Later, SNP (rs296887) of RMI1 was also identified to be associated with increased cancer risks for AML/MDS and MN, but not bladder cancer (118). The result from SNP studies of RMI1 is consistent with that from our mouse model, that RMI1 has potential function as a tumor suppressor gene. Taking together, RMI1, as a tumor suppressor gene, may have its potential applications in further cancer prevention and treatment.

Chapter IV

Conclusion and Future Directions

1.0 Conclusion

In this project, I have successfully established a knockout mouse model of RMI1 gene. I have shown that RMI1 is essential for early embryonic development.

Deleting both alleles of RMI1 leads to embryonic lethality before implantation. I have also demonstrated that whereas RMI1^{+/-} mice are viable and exhibit no obvious phenotypes, RMI1 heterozygosity, facilitates IR-induced tumor formations in p53^{+/-} background. The earlier onset and more progressive outcome of tumors from RMI1^{+/-}p53^{+/-} double-heterozygous mice suggest a potential role of RMI1 in tumor suppressing.

I have also investigated mechanisms of RMI1-associated cell death. Additional depleting of p53 restored colony formation ability of Rmi1 knockdown cells, indicating p53 and RMI1 are functionally related in regulating cellular viability. The exact mechanism of RMI1, however, needs further investigations.

2.0 Future Directions

2.1 Study molecular modification of RMI1

Post-transcriptional modification plays an important role in regulating protein activities. Among the three key components of the BTB complex, molecular modification on BLM has been studied extensively. BLM is phosphorylated at Thr⁹⁹ and Thr¹²² during mitosis and in response to genotoxic stress (20, 35, 37, 119). This phosphorylation is ATM/ATR dependent. Expression BLM^{T99G} and BLM^{T122A} in BS cells were able to restore normal frequency of SCE, but failed to correct radiosensitivity. BLM is also a substrate for SUMO modification (28). BLM mutations with abolished SUMO modification sites (K317 and K331) failed to localize to PML NBs, yet partially complemented the genomic instability phenotypes (120). It is possible that modifications may also be required for tight regulation of RMI1 activity.

Chang from our lab has identified Ser284 and Ser292 as two phosphorylation sites on Rmi1. Rmi1 is phosphorylated after UV, HU or IR treatment. This phosphorylation, unlike BLM's, is independent of ATM/ATR. Although the functional significance of RMI1 phosphorylation remains to be elucidated, it is of particular

interests to explore its role in coordinating RMI1 as well as BTB complex activity in response to DSBs. By utilizing the same strategy of RMI1 knockout, we could manage to establish a knock-in model of RMI1 with mutated phosphorylation site. This model, if available, would serve as the best tool to study function of RMI1 phosphorylation.

2.2 Study functional domains of RMI1

Structurally, several functional domains and evolutionary conserved regions have been identified in RMI1 protein. Whereas activity of certain domain remains controversial, the N-terminus of RMI1 is required for BLM and Topo3 α interactions. RMI1 mutations abolishing Topo3 α binding activity was unable to alleviate clonogenic survival of RMI1 depleted cells, suggesting a functional importance of this region. Despite recent progress, understanding of functions of other domains/regions is still limited. For example, RMI1 is proposed to recruiting BLM and Topo3 α onto DNA substrate and to facilitate their activity. However, the exact mechanism of Rmi1 in this process has yet identified. Further study on dissected functions of RMI1 by truncations or point mutations could illustrate RMI1 activity, and help us better reveal its function.

2.3 Study potential protein partners of RMI1

Physical and functional interactions between RMI1 and BLM/Topo3 α have been unfolded. Recently, the third protein binding to RMI1, RMI2, has been identified. Still, it is possible that potential RMI1-interacting proteins are yet to be found. Moreover, the kinase and phosphatase in response to Rmi1 phosphorylation remain unknown. Thus, searching for potential protein partners of Rmi1 would help in understanding RMI1 function and its exact role in BTB complex regulation.

2.4 Study RMI1 mutations/SNP in human cancers

Defective BLM causes Bloom syndrome. Since RMI1 is required for normal BLM function (82), its mutations may also lead to tumor-prone genetic disorders. However, several attempts have failed to detect such mutations. Recently, Broberg and co-workers have established RMI1 SNPs that associate with increased risk of cancers (117, 118). The two SNPs, locating at transcriptional and promoter regions of RMI1 respectively, are linked to a 2-fold increase of certain types of cancers. This finding, for the first time, established relationship between RMI1 and human cancer susceptibility. Together with our findings from irradiated RMI1^{+/-}p53^{+/-} mice, it is possible that polymorphisms or mutations of RMI1 could alter tumor risk and grade.

A high volume screening of RMI2 SNPs and mutations in tumor samples could further help us to reveal more information of cancer-associated RMI1 alleles. By studying these alleles, we may be able to learn dissected protein function/activity of Rmi1. Moreover, at least one SNP with increased cancer risk locates to the RMI1 promoter region. This SNP, as well as other potential ones, would help us to better understand the regulation of Rmi1 expression. Furthermore, these alleles could provide useful information in cancer prevention, diagnosis and treatment.

Bibliography

1. Chaganti RS, Houldsworth J. Fanconi anemia: a pleotropic mutation with multiple cellular and developmental abnormalities. *Ann Genet* 1991;34:206-11.
2. Hecht F, Hecht BK. Cancer in ataxia-telangiectasia patients. *Cancer Genet Cytogenet* 1990;46:9-19.
3. German J. Bloom syndrome: a mendelian prototype of somatic mutational disease. *Medicine (Baltimore)* 1993;72:393-406.
4. German J, Sanz MM, Ciocchi S, Ye TZ, Ellis NA. Syndrome-causing mutations of the BLM gene in persons in the Bloom's Syndrome Registry. *Hum Mutat* 2007;28:743-53.
5. Amor-Gueret M, Dubois-d'Enghien C, Lauge A, et al. Three new BLM gene mutations associated with Bloom syndrome. *Genet Test* 2008;12:257-61.
6. Ellis NA, Roe AM, Kozloski J, Proytcheva M, Falk C, German J. Linkage disequilibrium between the FES, D15S127, and BLM loci in Ashkenazi Jews with Bloom syndrome. *Am J Hum Genet* 1994;55:453-60.
7. Gruber SB, Ellis NA, Scott KK, et al. BLM heterozygosity and the risk of colorectal cancer. *Science* 2002;297:2013.
8. Cleary SP, Zhang W, Di Nicola N, et al. Heterozygosity for the BLM(Ash) mutation and cancer risk. *Cancer Res* 2003;63:1769-71.
9. Bachrati CZ, Hickson ID. RecQ helicases: guardian angels of the DNA replication fork. *Chromosoma* 2008;117:219-33.

10. Cheok CF, Bachrati CZ, Chan KL, Ralf C, Wu L, Hickson ID. Roles of the Bloom's syndrome helicase in the maintenance of genome stability. *Biochem Soc Trans* 2005;33:1456-9.
11. Liu Z, Macias MJ, Bottomley MJ, et al. The three-dimensional structure of the HRDC domain and implications for the Werner and Bloom syndrome proteins. *Structure* 1999;7:1557-66.
12. Bernstein DA, Zittel MC, Keck JL. High-resolution structure of the E.coli RecQ helicase catalytic core. *Embo J* 2003;22:4910-21.
13. Yu CE, Oshima J, Fu YH, et al. Positional cloning of the Werner's syndrome gene. *Science* 1996;272:258-62.
14. Kitao S, Shimamoto A, Goto M, et al. Mutations in RECQL4 cause a subset of cases of Rothmund-Thomson syndrome. *Nat Genet* 1999;22:82-4.
15. Macris MA, Krejci L, Bussen W, Shimamoto A, Sung P. Biochemical characterization of the RECQ4 protein, mutated in Rothmund-Thomson syndrome. *DNA Repair (Amst)* 2006;5:172-80.
16. Killoran MP, Keck JL. Sit down, relax and unwind: structural insights into RecQ helicase mechanisms. *Nucleic Acids Res* 2006;34:4098-105.
17. Wu L, Chan KL, Ralf C, et al. The HRDC domain of BLM is required for the dissolution of double Holliday junctions. *Embo J* 2005;24:2679-87.
18. Mohaghegh P, Karow JK, Brosh Jr RM, Jr., Bohr VA, Hickson ID. The Bloom's and Werner's syndrome proteins are DNA structure-specific helicases. *Nucleic Acids Res* 2001;29:2843-9.

19. Sun H, Karow JK, Hickson ID, Maizels N. The Bloom's syndrome helicase unwinds G4 DNA. *J Biol Chem* 1998;273:27587-92.
20. van Brabant AJ, Ye T, Sanz M, German IJ, Ellis NA, Holloman WK. Binding and melting of D-loops by the Bloom syndrome helicase. *Biochemistry* 2000;39:14617-25.
21. German J, Schonberg S, Louie E, Chaganti RS. Bloom's syndrome. IV. Sister-chromatid exchanges in lymphocytes. *Am J Hum Genet* 1977;29:248-55.
22. Imamura O, Fujita K, Itoh C, Takeda S, Furuichi Y, Matsumoto T. Werner and Bloom helicases are involved in DNA repair in a complementary fashion. *Oncogene* 2002;21:954-63.
23. Chester N, Kuo F, Kozak C, O'Hara CD, Leder P. Stage-specific apoptosis, developmental delay, and embryonic lethality in mice homozygous for a targeted disruption in the murine Bloom's syndrome gene. *Genes Dev* 1998;12:3382-93.
24. Wilson DM, 3rd, Thompson LH. Molecular mechanisms of sister-chromatid exchange. *Mutat Res* 2007;616:11-23.
25. Jacobson-Kram D, Albertini RJ, Branda RF, et al. Measurement of chromosomal aberrations, sister chromatid exchange, hprt mutations, and DNA adducts in peripheral lymphocytes of human populations at increased risk for cancer. *Environ Health Perspect* 1993;101 Suppl 3:121-5.
26. Luo G, Santoro IM, McDaniel LD, et al. Cancer predisposition caused by elevated mitotic recombination in Bloom mice. *Nat Genet* 2000;26:424-9.
27. Yankiwski V, Marciniak RA, Guarente L, Neff NF. Nuclear structure in normal and Bloom syndrome cells. *Proc Natl Acad Sci U S A* 2000;97:5214-9.

28. Beamish H, Kedar P, Kaneko H, et al. Functional link between BLM defective in Bloom's syndrome and the ataxia-telangiectasia-mutated protein, ATM. *J Biol Chem* 2002;277:30515-23.
29. Imamura O, Fujita K, Shimamoto A, et al. Bloom helicase is involved in DNA surveillance in early S phase in vertebrate cells. *Oncogene* 2001;20:1143-51.
30. Berg JM TJ, Stryer L, Clarke ND *Biochemistry*. ISBN 0-7167-3051-0. Chapter 27, Section 4: DNA Replication of Both Strands Proceeds Rapidly from Specific Start Sites.; 2002.
31. Lindahl T. The Croonian Lecture, 1996: endogenous damage to DNA. *Philos Trans R Soc Lond B Biol Sci* 1996;351:1529-38.
32. Samadashwily GM, Raca G, Mirkin SM. Trinucleotide repeats affect DNA replication in vivo. *Nat Genet* 1997;17:298-304.
33. Seigneur M, Bidnenko V, Ehrlich SD, Michel B. RuvAB acts at arrested replication forks. *Cell* 1998;95:419-30.
34. Turley H, Wu L, Canamero M, Gatter KC, Hickson ID. The distribution and expression of the Bloom's syndrome gene product in normal and neoplastic human cells. *Br J Cancer* 2001;85:261-5.
35. Bischof O, Kim SH, Irving J, Beresten S, Ellis NA, Campisi J. Regulation and localization of the Bloom syndrome protein in response to DNA damage. *J Cell Biol* 2001;153:367-80.
36. Sanz MM, Proytcheva M, Ellis NA, Holloman WK, German J. BLM, the Bloom's syndrome protein, varies during the cell cycle in its amount, distribution, and co-localization with other nuclear proteins. *Cytogenet Cell Genet* 2000;91:217-23.

37. Dutertre S, Ababou M, Onclercq R, et al. Cell cycle regulation of the endogenous wild type Bloom's syndrome DNA helicase. *Oncogene* 2000;19:2731-8.
38. Mullen JR, Kaliraman V, Brill SJ. Bipartite structure of the SGS1 DNA helicase in *Saccharomyces cerevisiae*. *Genetics* 2000;154:1101-14.
39. Cobb JA, Bjergbaek L, Shimada K, Frei C, Gasser SM. DNA polymerase stabilization at stalled replication forks requires Mec1 and the RecQ helicase Sgs1. *Embo J* 2003;22:4325-36.
40. Gangloff S, McDonald JP, Bendixen C, Arthur L, Rothstein R. The yeast type I topoisomerase Top3 interacts with Sgs1, a DNA helicase homolog: a potential eukaryotic reverse gyrase. *Mol Cell Biol* 1994;14:8391-8.
41. Ababou M, Dutertre S, Lecluse Y, Onclercq R, Chatton B, Amor-Gueret M. ATM-dependent phosphorylation and accumulation of endogenous BLM protein in response to ionizing radiation. *Oncogene* 2000;19:5955-63.
42. Hodges M, Tissot C, Howe K, Grimwade D, Freemont PS. Structure, organization, and dynamics of promyelocytic leukemia protein nuclear bodies. *Am J Hum Genet* 1998;63:297-304.
43. Wang XW, Tseng A, Ellis NA, et al. Functional interaction of p53 and BLM DNA helicase in apoptosis. *J Biol Chem* 2001;276:32948-55.
44. Zhong S, Hu P, Ye TZ, Stan R, Ellis NA, Pandolfi PP. A role for PML and the nuclear body in genomic stability. *Oncogene* 1999;18:7941-7.
45. Yankiwski V, Noonan JP, Neff NF. The C-terminal domain of the Bloom syndrome DNA helicase is essential for genomic stability. *BMC Cell Biol* 2001;2:11.

46. Davalos AR, Kaminker P, Hansen RK, Campisi J. ATR and ATM-dependent movement of BLM helicase during replication stress ensures optimal ATM activation and 53BP1 focus formation. *Cell Cycle* 2004;3:1579-86.
47. Pages V, Fuchs RP. Uncoupling of leading- and lagging-strand DNA replication during lesion bypass in vivo. *Science* 2003;300:1300-3.
48. Higuchi K, Katayama T, Iwai S, Hidaka M, Horiuchi T, Maki H. Fate of DNA replication fork encountering a single DNA lesion during oriC plasmid DNA replication in vitro. *Genes Cells* 2003;8:437-49.
49. Lopes M, Cotta-Ramusino C, Pellicioli A, et al. The DNA replication checkpoint response stabilizes stalled replication forks. *Nature* 2001;412:557-61.
50. Heller RC, Marians KJ. Replisome assembly and the direct restart of stalled replication forks. *Nat Rev Mol Cell Biol* 2006;7:932-43.
51. Heller RC, Marians KJ. The disposition of nascent strands at stalled replication forks dictates the pathway of replisome loading during restart. *Mol Cell* 2005;17:733-43.
52. Ralf C, Hickson ID, Wu L. The Bloom's syndrome helicase can promote the regression of a model replication fork. *J Biol Chem* 2006;281:22839-46.
53. Longhese MP, Clerici M, Lucchini G. The S-phase checkpoint and its regulation in *Saccharomyces cerevisiae*. *Mutat Res* 2003;532:41-58.
54. Sclafani RA, Holzen TM. Cell cycle regulation of DNA replication. *Annu Rev Genet* 2007;41:237-80.
55. Franchitto A, Pichierri P. Bloom's syndrome protein is required for correct relocalization of RAD50/MRE11/NBS1 complex after replication fork arrest. *J Cell Biol* 2002;157:19-30.

56. Wang Y, Cortez D, Yazdi P, Neff N, Elledge SJ, Qin J. BASC, a super complex of BRCA1-associated proteins involved in the recognition and repair of aberrant DNA structures. *Genes Dev* 2000;14:927-39.
57. Davalos AR, Campisi J. Bloom syndrome cells undergo p53-dependent apoptosis and delayed assembly of BRCA1 and NBS1 repair complexes at stalled replication forks. *J Cell Biol* 2003;162:1197-209.
58. Garkavtsev IV, Kley N, Grigorian IA, Gudkov AV. The Bloom syndrome protein interacts and cooperates with p53 in regulation of transcription and cell growth control. *Oncogene* 2001;20:8276-80.
59. Sengupta S, Linke SP, Pedoux R, et al. BLM helicase-dependent transport of p53 to sites of stalled DNA replication forks modulates homologous recombination. *Embo J* 2003;22:1210-22.
60. Sengupta S, Robles AI, Linke SP, et al. Functional interaction between BLM helicase and 53BP1 in a Chk1-mediated pathway during S-phase arrest. *J Cell Biol* 2004;166:801-13.
61. Cong YS, Wright WE, Shay JW. Human telomerase and its regulation. *Microbiol Mol Biol Rev* 2002;66:407-25, table of contents.
62. Royle NJ, Foxon J, Jeyapalan JN, et al. Telomere length maintenance--an ALternative mechanism. *Cytogenet Genome Res* 2008;122:281-91.
63. Tanaka H, Mendonca MS, Bradshaw PS, et al. DNA damage-induced phosphorylation of the human telomere-associated protein TRF2. *Proc Natl Acad Sci U S A* 2005;102:15539-44.
64. Broccoli D, Smogorzewska A, Chong L, de Lange T. Human telomeres contain two distinct Myb-related proteins, TRF1 and TRF2. *Nat Genet* 1997;17:231-5.

65. Fairall L, Chapman L, Moss H, de Lange T, Rhodes D. Structure of the TRFH dimerization domain of the human telomeric proteins TRF1 and TRF2. *Mol Cell* 2001;8:351-61.
66. Lillard-Wetherell K, Machwe A, Langland GT, et al. Association and regulation of the BLM helicase by the telomere proteins TRF1 and TRF2. *Hum Mol Genet* 2004;13:1919-32.
67. Stavropoulos DJ, Bradshaw PS, Li X, et al. The Bloom syndrome helicase BLM interacts with TRF2 in ALT cells and promotes telomeric DNA synthesis. *Hum Mol Genet* 2002;11:3135-44.
68. Seki M, Nakagawa T, Seki T, et al. Bloom helicase and DNA topoisomerase IIIalpha are involved in the dissolution of sister chromatids. *Mol Cell Biol* 2006;26:6299-307.
69. McVey M, Andersen SL, Broze Y, Sekelsky J. Multiple functions of Drosophila BLM helicase in maintenance of genome stability. *Genetics* 2007;176:1979-92.
70. Chan KL, North PS, Hickson ID. BLM is required for faithful chromosome segregation and its localization defines a class of ultrafine anaphase bridges. *Embo J* 2007;26:3397-409.
71. Podhorecka M. [gamma H2AX in the recognition of DNA double-strand breaks]. *Postepy Hig Med Dosw (Online)* 2009;63:92-8.
72. Greenberg RA. Recognition of DNA double strand breaks by the BRCA1 tumor suppressor network. *Chromosoma* 2008;117:305-17.
73. Pardo B, Gomez-Gonzalez B, Aguilera A. DNA repair in mammalian cells: DNA double-strand break repair: how to fix a broken relationship. *Cell Mol Life Sci* 2009;66:1039-56.

74. Lieber MR. The mechanism of human nonhomologous DNA end joining. *J Biol Chem* 2008;283:1-5.
75. Sung P, Klein H. Mechanism of homologous recombination: mediators and helicases take on regulatory functions. *Nat Rev Mol Cell Biol* 2006;7:739-50.
76. Wyman C, Ristic D, Kanaar R. Homologous recombination-mediated double-strand break repair. *DNA Repair (Amst)* 2004;3:827-33.
77. Poplawski T, Blasiak J. [DNA homologous recombination repair in mammalian cells]. *Postepy Biochem* 2006;52:180-93.
78. Bachrati CZ, Hickson ID. RecQ helicases: suppressors of tumorigenesis and premature aging. *Biochem J* 2003;374:577-606.
79. Plank JL, Wu J, Hsieh TS. Topoisomerase IIIalpha and Bloom's helicase can resolve a mobile double Holliday junction substrate through convergent branch migration. *Proc Natl Acad Sci U S A* 2006;103:11118-23.
80. Sung P, Krejci L, Van Komen S, Sehorn MG. Rad51 recombinase and recombination mediators. *J Biol Chem* 2003;278:42729-32.
81. Bugreev DV, Yu X, Egelman EH, Mazin AV. Novel pro- and anti-recombination activities of the Bloom's syndrome helicase. *Genes Dev* 2007;21:3085-94.
82. Yin J, Sobeck A, Xu C, et al. BLAP75, an essential component of Bloom's syndrome protein complexes that maintain genome integrity. *Embo J* 2005;24:1465-76.
83. Karow JK, Constantinou A, Li JL, West SC, Hickson ID. The Bloom's syndrome gene product promotes branch migration of holliday junctions. *Proc Natl Acad Sci U S A* 2000;97:6504-8.

84. Meetei AR, Sechi S, Wallisch M, et al. A multiprotein nuclear complex connects Fanconi anemia and Bloom syndrome. *Mol Cell Biol* 2003;23:3417-26.
85. D'Andrea AD, Grompe M. The Fanconi anaemia/BRCA pathway. *Nat Rev Cancer* 2003;3:23-34.
86. Mullen JR, Nallaseth FS, Lan YQ, Slagle CE, Brill SJ. Yeast Rmi1/Nce4 controls genome stability as a subunit of the Sgs1-Top3 complex. *Mol Cell Biol* 2005;25:4476-87.
87. Chang M, Bellaoui M, Zhang C, et al. RMI1/NCE4, a suppressor of genome instability, encodes a member of the RecQ helicase/Topo III complex. *Embo J* 2005;24:2024-33.
88. Singh TR, Ali AM, Busygina V, et al. BLAP18/RMI2, a novel OB-fold-containing protein, is an essential component of the Bloom helicase-double Holliday junction dissolvosome. *Genes Dev* 2008;22:2856-68.
89. Xu D, Guo R, Sobeck A, et al. RMI, a new OB-fold complex essential for Bloom syndrome protein to maintain genome stability. *Genes Dev* 2008;22:2843-55.
90. Champoux JJ. DNA topoisomerases: structure, function, and mechanism. *Annu Rev Biochem* 2001;70:369-413.
91. Leppard JB, Champoux JJ. Human DNA topoisomerase I: relaxation, roles, and damage control. *Chromosoma* 2005;114:75-85.
92. Slesarev AI, Stetter KO, Lake JA, Gellert M, Krah R, Kozyavkin SA. DNA topoisomerase V is a relative of eukaryotic topoisomerase I from a hyperthermophilic prokaryote. *Nature* 1993;364:735-7.
93. Pourquier P, Pommier Y. Topoisomerase I-mediated DNA damage. *Adv Cancer Res* 2001;80:189-216.

94. Brown PO, Cozzarelli NR. Catenation and knotting of duplex DNA by type 1 topoisomerases: a mechanistic parallel with type 2 topoisomerases. *Proc Natl Acad Sci U S A* 1981;78:843-7.
95. Chakraverty RK, Kearsey JM, Oakley TJ, et al. Topoisomerase III acts upstream of Rad53p in the S-phase DNA damage checkpoint. *Mol Cell Biol* 2001;21:7150-62.
96. Gangloff S, de Massy B, Arthur L, Rothstein R, Fabre F. The essential role of yeast topoisomerase III in meiosis depends on recombination. *Embo J* 1999;18:1701-11.
97. Win TZ, Goodwin A, Hickson ID, Norbury CJ, Wang SW. Requirement for *Schizosaccharomyces pombe* Top3 in the maintenance of chromosome integrity. *J Cell Sci* 2004;117:4769-78.
98. Shor E, Gangloff S, Wagner M, Weinstein J, Price G, Rothstein R. Mutations in homologous recombination genes rescue top3 slow growth in *Saccharomyces cerevisiae*. *Genetics* 2002;162:647-62.
99. Oakley TJ, Goodwin A, Chakraverty RK, Hickson ID. Inactivation of homologous recombination suppresses defects in topoisomerase III-deficient mutants. *DNA Repair (Amst)* 2002;1:463-82.
100. Laursen LV, Ampatzidou E, Andersen AH, Murray JM. Role for the fission yeast RecQ helicase in DNA repair in G2. *Mol Cell Biol* 2003;23:3692-705.
101. Goulaouic H, Roulon T, Flamand O, Grondard L, Lavelle F, Riou JF. Purification and characterization of human DNA topoisomerase III α . *Nucleic Acids Res* 1999;27:2443-50.

102. Temime-Smaali N, Guittat L, Wenner T, et al. Topoisomerase IIIalpha is required for normal proliferation and telomere stability in alternative lengthening of telomeres. *Embo J* 2008;27:1513-24.
103. Wu L, Bachrati CZ, Ou J, et al. BLAP75/RMI1 promotes the BLM-dependent dissolution of homologous recombination intermediates. *Proc Natl Acad Sci U S A* 2006;103:4068-73.
104. Raynard S, Zhao W, Bussen W, et al. Functional role of BLAP75 in BLM-topoisomerase IIIalpha-dependent holliday junction processing. *J Biol Chem* 2008;283:15701-8.
105. Mankouri HW, Hickson ID. The RecQ helicase-topoisomerase III-Rmi1 complex: a DNA structure-specific 'dissolvasome'? *Trends Biochem Sci* 2007;32:538-46.
106. Henning W, Sturzbecher HW. Homologous recombination and cell cycle checkpoints: Rad51 in tumour progression and therapy resistance. *Toxicology* 2003;193:91-109.
107. Wu L. Role of the BLM helicase in replication fork management. *DNA Repair (Amst)* 2007;6:936-44.
108. Raynard S, Bussen W, Sung P. A double Holliday junction dissolvasome comprising BLM, topoisomerase IIIalpha, and BLAP75. *J Biol Chem* 2006;281:13861-4.
109. Wu L, Hickson ID. The Bloom's syndrome helicase suppresses crossing over during homologous recombination. *Nature* 2003;426:870-4.
110. Bussen W, Raynard S, Busygina V, Singh AK, Sung P. Holliday junction processing activity of the BLM-Topo IIIalpha-BLAP75 complex. *J Biol Chem* 2007;282:31484-92.

111. Goss KH, Risinger MA, Kordich JJ, et al. Enhanced tumor formation in mice heterozygous for Blm mutation. *Science* 2002;297:2051-3.
112. Li W, Wang JC. Mammalian DNA topoisomerase IIIalpha is essential in early embryogenesis. *Proc Natl Acad Sci U S A* 1998;95:1010-3.
113. Marez D, Legrand M, Sabbagh N, et al. Polymorphism of the cytochrome P450 CYP2D6 gene in a European population: characterization of 48 mutations and 53 alleles, their frequencies and evolution. *Pharmacogenetics* 1997;7:193-202.
114. Brookes AJ. The essence of SNPs. *Gene* 1999;234:177-86.
115. London SJ, Lehman TA, Taylor JA. Myeloperoxidase genetic polymorphism and lung cancer risk. *Cancer Res* 1997;57:5001-3.
116. Golka K, Prior V, Blaszkewicz M, Bolt HM. The enhanced bladder cancer susceptibility of NAT2 slow acetylators towards aromatic amines: a review considering ethnic differences. *Toxicol Lett* 2002;128:229-41.
117. Broberg K, Hoglund M, Gustafsson C, et al. Genetic variant of the human homologous recombination-associated gene RMI1 (S455N) impacts the risk of AML/MDS and malignant melanoma. *Cancer Lett* 2007;258:38-44.
118. Broberg K, Huynh E, Schlawicke Engstrom K, et al. Association between polymorphisms in RMI1, TOP3A, and BLM and risk of cancer, a case-control study. *BMC Cancer* 2009;9:140.
119. Ababou M, Dumaire V, Lecluse Y, Amor-Gueret M. Bloom's syndrome protein response to ultraviolet-C radiation and hydroxyurea-mediated DNA synthesis inhibition. *Oncogene* 2002;21:2079-88.

120. Eladad S, Ye TZ, Hu P, et al. Intra-nuclear trafficking of the BLM helicase to DNA damage-induced foci is regulated by SUMO modification. *Hum Mol Genet* 2005;14:1351-65.

Protein Interaction Network among INO80 Complex Subunits

Introduction & Significance

1.0 Classification of chromatin remodeling complexes

The genomic DNA of eukaryotic cells is packaged into highly compacted and stable chromatin structure, which helps to envelop it in the nucleus. The primary unit of the chromatin structure is the nucleosome. It includes 146 base pairs of DNA, which wraps about 1.7 left-handed turns around the histone octamer composed of two H2A-H2B heterodimers and one H3-H4 tetramer. During genomic DNA packaging process, it could be packaged into higher order structures termed chromatin fibers.

Although nucleosomal structure alleviates the spatial constrain of the nucleus, this compacted structure presents a barrier for proper DNA metabolic processes, as these processes are impeded due to limited accessibility of DNA substrates. In order to create dynamic chromatin environment and expose desired DNA substrates, chromatin structure are reconfigured by two distinct yet highly intertwined mechanisms, post-translational modification of histones and ATP-dependent chromatin remodeling (121, 122) (**Table 1, 2.**).

The ATP-dependent chromatin remodeling complexes are named after their ATPase subunits, all of which belong to the SWI/SNF family, a part of SNF2 superfamily. These subunits could be further divided into subfamilies, including the SWI/SNF, ISWI, CHD and INO80 (**Table 2.**). Among them, the INO80 subfamily is the most recent identified family, which is conserved from yeast to mammals (123).

Classes of histone modification	Histone-modifying enzymes and binding partners involved in cancer		Cellular defects and/or deregulation observed in cancer
'Writers' – HMTs	H3K4	MLL	Tumor promotion Transcription regulation; oncogenic fusion proteins of MLL; amplification; tandem duplication in AML, ALL and MDS
		SMYD3	Tumor promotion Transcription regulation; cell-cycle defects; upregulation in colorectal and haptocellular carcinoma cell lines; overexpression in cell lines promotes cell growth and transformation
	H3K9	SUV39H1	Tumor suppression Cell-cycle defects; chromosome instability; transcription regulation; B cell lymphoma in knockout mice (mouse model); no known mutations reported in human cancers yet
		RIZ1/PRDM2	Tumor suppression Transcription regulation; frame shift, missense mutations and epigenetic silencing; LOH in human hepatocellular carcinoma, colon, melanoma, sarcoma, breast and gastric cancers; B cell lymphoma and stomach cancer in mouse model
	H3K27	EZH2	Tumor promotion Cell-cycle defects; overexpression and amplification in human prostate cancer, breast cancer, lymphoma, myeloma, colorectal cancer, endometrial cancer, bladder cancer and melanoma
	H3K36	NSD1	Tumor suppression Heterozygous germline mutations in Sotos syndrome increases risk for human hepatocellular carcinoma, leukemia and neuroblastoma
	H3K79	hDOT1L	Tumor promotion Transcription regulation; leukemogenesis in association with AF10 fusion proteins
	'Readers'	H3K4	INGs Tumor suppression Transcription regulation; DNA-damage repair; DNA replication; mutations, LOH and downregulation in breast cancer, gastric cancer, melanoma, glioma, and head and neck squamous cell carcinoma
		H3K9	HP1 Tumor suppression Transcription regulation; frame shift, missense mutations and epigenetic silencing; LOH in human hepatocellular carcinoma, colon, melanoma, sarcoma, breast and gastric cancers; B-cell lymphoma and stomach cancer in mouse model
		H3K27	BM11/PRC1 Tumor promotion Cell-cycle defects; overexpression in lymphoma, leukemia, medulloblastoma, neuroblastoma and NSCLC
'Erasers' – Demethylases	H3K9	JMJD2C/GASC1	Tumor promotion
	H3K36		Promotes AR-dependent transcription and prostate cancer cell proliferation; overexpressed in human esophageal squamous cell carcinoma, lung sarcomatoid carcinoma and desmoplastic medulloblastoma

2.0

Table 1. List of covalent histone modifications.
Adapted from Gang C. Wang, C. David Allis, Ping Chi,
Chromatin remodeling and cancer, Part I: covalent
histone modifications., Trends in Molecular Medicines,
Volume 13, Issue 9, September 2007, Pages 363-372.

Family and complexes	Remodeling-complex subunits	Complex functions
SWI/SNF family		
BAF	BRM or BRG1, SNF5/INI1, BAF155, BAF170, BAF250, BAF53, β -actin, BAF60a, BAF57	Tumor suppressor, cell-cycle progression, DNA replication, development, differentiation, elongation, signaling, splicing, DNA-damage repair
PBAF	BRG1, SNF5/INI1, BAF155, BAF170, BAF180, BAF53, β -actin, BAF60a	
BRM	BRM, SNF5/INI1, BAF155, BAF170, BAF250, BAF53, BAF60a	
BRG1-complex I	BRG1, SNF5/INI1, BAF155, BAF170, BAF250, BAF53, BAF60a	
BRG1-complex II	BRG1, SNF5/INI1, BAF155, BAF170, BAF250, BAF53	
EBAFa	BRG1, SNF5/INI1, BAF155, BAF170, BAF250a, BAF53, β -actin, BAF60a, ENL, EBAF70, EBAF100, EBAF140	
EBAFb	BRG1, SNF5/INI1, BAF155, BAF170, BAF250b, BAF53, β -actin, BAF60b, ENL, EBAF70, EBAF100, EBAF140	
ISWI family		
ACF/WCRF	SNF2H, WCRF180/ACF1	X-chromosome regulation, cohesion, embryonic development and differentiation, transcriptional activation and repression, DNA replication, DNA repair response
CHRAC	SNF2H, ACF1, CHRAC17, CHRAC15	
RSF	SNF2H, p325	
WICH	SNF2H, WSTF	
SNF2H/Cohesin	SNF2H, Mi-2, Rad21, HDAC1, HDAC2, MTA1, MTA2, SA1/SA2, RbAp46, RbAp48, MBD2, MBD3, SMC1, SMC3	
NURF	SNF2L, BPTF, RbAp46, RbAp48	
NURD/Mi-2/CHD family		
NuRD/Mi-2/CHD	Mi2- α /CHD3 or Mi2- β /CHD4 or CHD1-2 or CHD5, HDAC1, HDAC2, RbAp46, RbAp48, MTA1 or MTA2 or MTA3, MBD2 or MBD3	Tumor suppressor, transcriptional repression and silencing, transcriptional activation, pluripotency of embryonic stem cell
INO80 family		
INO80	hINO80, Tip49a, Tip49b, BAF53a, Arp5, Arp8, hles2, hles6, Amida, NFRKB, MCRS1, FLJ90652, FLJ20309	
TRRAP/Tip60	P400, Tip49a, Tip49b, BAF53a, actin, GAS41, DMAP1, YL-1, Brd8, TRRAP, Tip60, MRG15, MRGX, FLJ11730, MRGBP, EPC1, ING3	
SRCAP	SRCAP, Tip49a, Tip49b, BAF53a, Arp6, GAS41, DAMP1, YL-1, ZnF-HIT1	

Table 2. List of ATP-dependent chromatin remodeling complexes. Adapted from Gang C. Wang, C. David Allis, Ping Chi, Chromatin remodeling and cancer, Part II: ATP-dependent chromatin remodeling., Trends in Molecular Medicines, Volume 13, Issue 9, September 2007, Pages 373-380.

2.0 Cellular functions of INO80 complex

Previous studies have indicated that INO80 complex is involved in almost all DNA metabolic processes, which include transcription, replication, and damage repair. Interestingly, INO80 complex may also have function in checkpoint regulation (124). In the following sections, INO80 complex function in different DNA metabolic processes will be discussed briefly.

2.1 The INO80 complex in transcriptional regulation

The Ino80 ATPase was first identified as a transcriptional regulator. Initial characterization suggested that it was required for inositol-responsive gene expression (125). Later, evidences indicate that this protein, as well as its complex, in response to a variety of signaling pathways, is able to regulate a limited set of gene transcriptions in yeast, plants and mammals (126-128).

The function of INO80 complex in transcription regulation associates with transcription factor YY1, which is an interaction protein of the human INO80 complex (**Figure 3.**). Cai, Y et al. demonstrated that the INO80 complex is required for YY1 binding to two well-characterized YY1-activated genes, and deleting two subunits of INO80 complex abolishes expressions of these two genes (128).

2.2 The INO80 complex in DNA replication

Several recent studies have suggested that INO80 complex contributes to ensuring replication fork progress during both normal and challenged situations. Yeast INO80 complex is recruited onto not only normal non-stressed, but also stalled replication forks and unfired replication origins, both of which are induced by HU (126, 129, 130). Moreover, yeast strains with mutations of INO80 subunits exhibit a slower growth phenotype (130), suggesting a defective DNA replication in the absence of INO80 complex. Further studies show these strains are unable to efficiently restart replication after stress and accumulate DSB, mainly due to dissociation of replication machinery from stalled replication forks (126, 129). Based on these correlative evidence, INO80 complex is proposed to promote remodeling or remove nucleosomes in the path of replication forks, and possibly, reassembling them after strand synthesis. However, this proposed mechanism of INO80 complex in DNA replication remains to be proved.

2.3 The INO80 complex in DNA repair

Deletions or mutations of INO80 complex subunits are hypersensitive to a variety of reagents causing DNA damage, including methylmethane sulfate (MMS), ionizing radiation (IR), ultraviolet (UV) and topoisomerase inhibitors (131, 132). These observations indicate that the INO80 complex has a function in DNA repair.

Recently, progress has been made in understanding the INO80 complex's role in DSB repair. Yeast INO80 complex is known to be recruited to the vicinity of HO-induced DSB within 2 hours. This recruitment is partially dependent on phospho-H2A, since deletion of H2A is able to reduce this recruitment (133, 134). Further investigations indicate that Arp4 and Nhp10, two subunits of INO80 complex, contribute to phospho-H2A recognition. Deletion of either gene in yeast results in reduced recruitment of INO80 complex subunits to DSBs (135). However, it is still debatable whether Arp4 is dispensable in this recruitment, as it is reported that INO80 complex stably binds to γ -H2AX in the absence of Arp4 (135).

Moreover, in mammalian cells, INO80 complex is associated with HR-mediated DSB repairs. Depletion of either Ino80 or YY1 leads to substantial reduced HR activity (132). The mechanism under this observation, however, needs further investigation.

In addition, INO80 complex may have its function in checkpoint response. Deleting IES4, a subunit of yeast INO80 complex, leads to depressed p53 activation. In contrast, phosphor-mimic mutant of this gene exhibits enhanced p53 activation and slower S phase progression with MMS, whereas the repair machinery appears normally (136, 137).

3.0 Protein Components of INO80 Complex

The human INO80 complex was first isolated by the J Conaway laboratory (128, 137). Among the 15 subunits identified from this complex, 8 are orthologs of yeast INO80 complex components. Because of their functional importance and evolutionary conservation, hereafter, these 8 proteins are referred as core subunits of INO80 complex. Moreover, 3 subunits, INO80, Arp5 and Arp8, are presented exclusively in this complex, and are not found in other chromatin remodeling complexes. (**Table 3.**). Although the role of INO80 complex in DNA metabolism is implicated, functions of individual INO80 subunits, other than the ATPase-helicase components Ino80, remain largely elusive.

The Ino80 protein is generally considered as the key factor in this complex (**Figure 1.**). First, although it is not the only ATPase within this complex, its ATP hydrolysis activity is required for this complex's chromatin remodeling function (125, 131). Second, Ino80 has physical interactions with several core INO80 complex subunits, including actin, actin-related proteins (Arps) and Rvbs (124). Thus it may serve as a docking station of INO80 complex (**Figure 1.**).

Yeast	Human	Domain structure
Ino80p	INO80	Snf-2like ATPase
Actin	B-actin	
Arp4p	Baf53a (Arp4)	Actin-related protein
Arp5p	Arp5	Actin-related protein
Arp8p	Arp8	Actin-related protein
Rvb1p	RuvB-like 1 (Tip49a)	AAA+ ATPases
Rvb2p	RuvB-like 2 (Tip49b)	AAA+ ATPases
Ies2p	Ies2 (PAPA-1)	Zinc finger-HIT domain
Ies6p	Ies6 (c18orf37)	
Nhp10p	-	HMG type-II domain
Taf14p	-	
Ies1p	-	
Ies3p	-	
Ies4p	-	
Ies5p	-	
-	YY1	GLI-Kruppel zinc finger transcription factor
-	Uch37	
-	NFRKB	UCH family deubiquitylating enzyme
-	MCRS1	
-	TFPT	FHA domain
-	INO80D (FLJ20309)	
-	INO80E (CCDC95)	Coiled-coil domain

Table 3. Subunits of budding yeast and human INO80 complexes. Subunits of INO80 complexes are listed. A dash (-) indicates absence of ortholog in the complex. Adapted and modified from Ronald C. Conaway and Joan W. Conaway, The INO80 chromatin remodeling complex in transcription, replication and repair., Trends in Biochemical Sciences, Volume 34, Issue 2, February 2009, Pages 71-77.

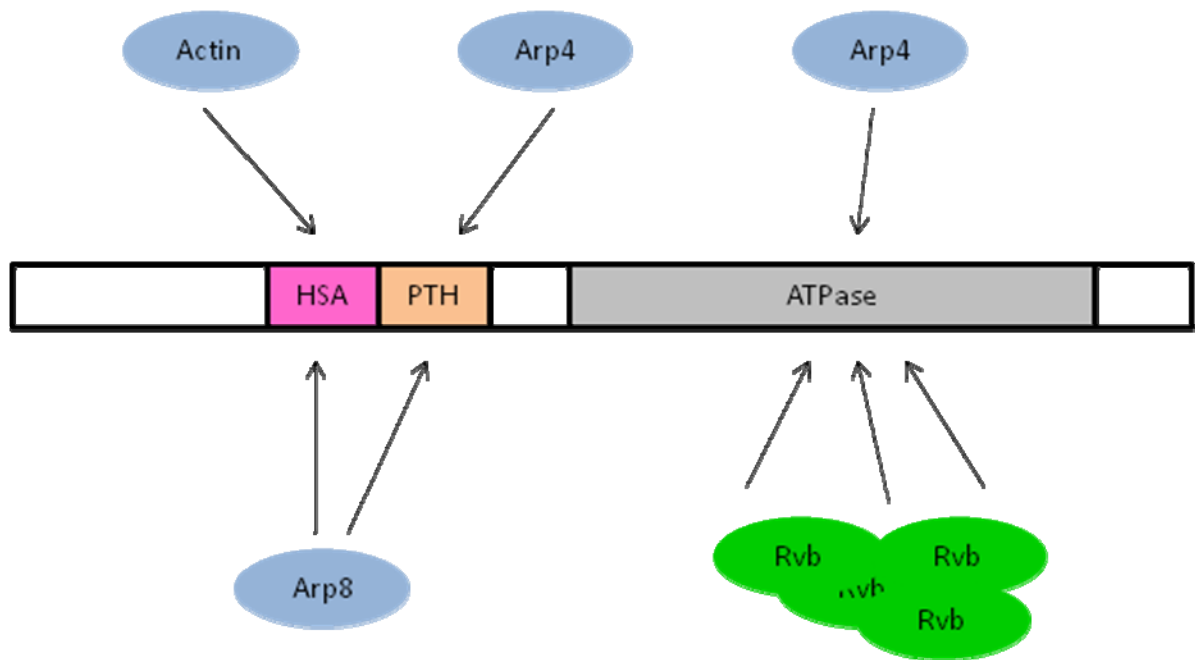


Figure 1. Known domains and interactions of Ino80 protein. HSA (pink) and PTH (post-HSA, light blue) domains are required for Actin and Arp4 (green) binding, respectively. The ATPase domain (gray) of Ino80 is split by an insertion, which is required for Arp5 (green) and Rvb binding (light green).

The AAA⁺ ATPases Rvb1 and Rvb2 are evolutionarily conserved from yeast to human, which shares sequence similarity to bacterial RuvB ATPase (138).

Structurally, the Rvb1/Rvb2 forms two stacked hexameric rings with 6 of each protein (139, 140). Nevertheless, it is unclear whether these two proteins integrate into INO80 complex with similar structure, although IP assays suggest they keep six-fold stoichiometry in INO80 complexes from both yeast and human (128, 131).

Although the exact function remains unknown, Rvb proteins may be required for stable assembly of INO80 complex, as Rvb2 is required for recruitment of Arp5 to the site of DNA double strand breaks (141).

Ino80 interacts with multiple Actin and Actin-related proteins, including Arp4, Arp5 and Arp8 (137). The docking sites of these proteins on Ino80 have been mapped. As previously described, Arp5 and Arp8 are specifically presented in INO80 complex. Based on observations of Arp-histone bindings, it is proposed that these Actin-related proteins may contribute to nucleosome binding of INO80 complex (142, 143). Protein interactions and their functions between other components of the INO80 complex remains unknown. Identification of these interactions will provide additional understanding toward the INO80 complex structure and function.

4.0 Bimolecular fluorescence complementation assay

The Bimolecular fluorescence complementation (BiFC) assay, first reported by Hu CD et al. in 2002, is designed to detect protein-protein association in living cells (144). In this assay, two putative interacting proteins were fused with non-functional fluorescent protein fragments, respectively (**Figure 2.**). If taken into close distance, the two fragments are able to resemble themselves and reconstitute functional fluorophore. The fluorescent signal then could be visualized under microscopy, which indicates the physical interaction of proteins. Comparing with traditional *in vitro* interaction assays, BiFC is able to provide visualized images of interaction with native proteins.

5.0 Goals of experiment

Despite that the core components of the INO80 complex have been identified and some of the structure features of this complex have been revealed, the detailed information of *in vivo* protein-protein interaction within this complex remains unknown. Furthermore, functional study of its core subunits, especially, the

biological function of nuclear ARPs in maintaining complex stability, needs further investigation.

In this study, I investigate protein-protein interactions among the 7 conserved core subunits of human INO80 complex using the BiFC assay. This experiment will provide a comprehensive view of physical protein contact within the INO80 complex. In addition, our lab has successfully developed Ino80 and Arp5 somatic conditional knockout cell strains. In combination with these mutant strains, we may be able to reveal Ino80 and Arp5's function in maintaining stability of INO80 complex.

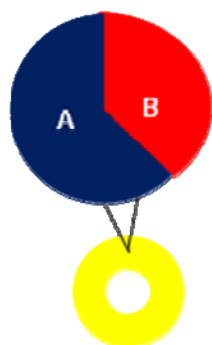
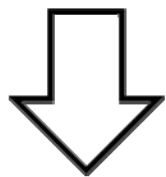
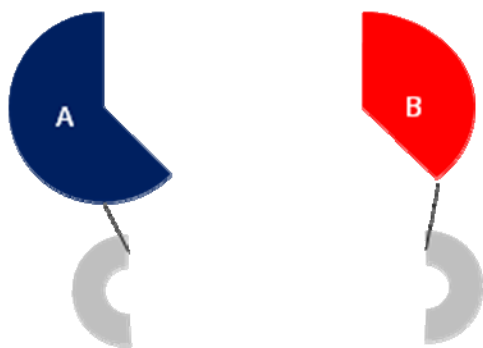


Figure 2. Principle of BiFC assay. The YFP protein is divided into two nonfunctional fragments (Gray half-circles)(1-154 and 155-238, or N- and C-terminal fragments, respectively), and fused to two proteins (A & B, respectively). If the two proteins interact with each other, it could bring two YFP fragments into close vicinity, where the two fragments are able to reassemble functional YFP and be visualized under standard epifluorescence microscope (Yellow circle).

Materials and Methods

1.0 Cell Culture and cDNA Cloning/Transfection

HEK293 and HEK293T cell lines were culture in DMEM medium, supplemented with 10% FBS. Cells were incubated in 37°C incubator with 5.5% CO₂ concentration.

cDNA of Arp4, Tip49a, Tip49b and les6 were obtained from Human ORFeome V3.1 program, from which all cDNA was cloned into Gateway pDOR223 vector. The plate numbers of 4 hORFeome cDNA clones are listed below: Arp4, D01-11037; Rvb1, H06-11011; Rvb2, D01-11037; les6, D01-31001. cDNA of les2, Arp5 and Arp8 were amplified by PCR and cloned into pDOR201 vector, respectively. The PCR primers used in cDNA amplications were listed below: Arp5 upper,

ggggacaactttgtacaaaaaagttggcatggcgccgaacgtgttt; Arp5 lower, ggggacaactttgtacaagaaagttgggtatgcctgctcaccagcac; Arp8 upper, ggggacaactttgtacaaaaaagttggcatgacccaggctgagaag; Arp8 lower, ggggacaactttgtacaagaaagttgggcaccacacaaacgcagcc; les2 upper, ggggacaactttgtacaaaaaagttggcatggaggcccctgagccg; les2 lower, ggggacaactttgtacaagaaagttgggtacgtagccaaaagggg.

cDNAs carried by pENTRY vector were transferred into 4 pBABE-based destination vectors (pB-CMV-DEST-VN-neo, pB-CMV-VN-DEST-neo, pB-CMV-DEST-YFPC-

puro and pB-CMV-YFPC-DEST-puro, respectively) in LR reaction. Expression plasmids were transfected into HEK 293 or HEK293T cells with Fugen6.

2.0 Immunoblotting and Green Fluorescent Signal Detection

Proteins were separated by 8% SDS/PAGE gel. C- and N-terminal GFP fragment tagged INO80 subunits were detected by incubating with polyclonal anti-GFP antibody (SC-9996) overnight at 4°C. For green fluorescent signal detection, cells transiently transfected with expression plasmids were cultured on cover slips until reaching confluence. Slips were then carefully washed with PBS, incubated with 4% paraformaldehyde for 10 minutes and fixed with 0.5% triton solution for 15 minutes in R.T. before mounted on glass slides and visualized under fluorescence microscope (Leica DM4000B).

Results

1.0 Constructions and expressions of YFP-tagged INO80 subunits

In order to explore molecular structure of INO80 complex, I performed BiFC assay to study protein-protein interactions within this complex. 7 core subunits of this complex were selected for this assay, including Arp4, Arp5, Arp8, Rvb1, Rvb2, Ies2 and Ies6. All of them are orthologs of yeast INO80 complex core components. Specially, Arp5 and Arp8 are exclusively presented in INO80 complex.

cDNA of 7 INO80 subunits were each separately cloned into 4 distinct destination vectors, which fuse C- or N-terminal venus YFP fragment at either end of targeted protein, respectively. These expression constructs were next transfected into HEK293 cells. Twenty hours after transfection, cells were collected for western blots against a polyclonal anti-GFP antibody, which is capable of detecting YFP. As shown in **Figure 3**, expressions of 4 versions of fusion proteins from 7 subunits were detected.

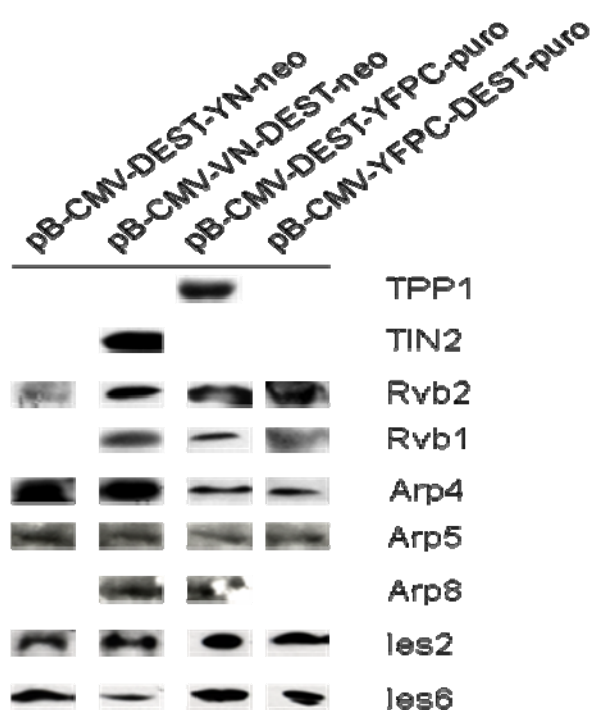


Figure 3. Western blots for YFP fragments tagged INO80 complex subunits. Each subunit was cloned into four different destination vectors with C- or N- terminal fragment venus YFP attached either end of subunit, respectively. TPP1 and TIN2 fusion proteins were used as positive controls.

2.0 Fluorescence microscopy

To detect all potential protein-protein interactions among the 7 targeted subunits, I cross-tested all possible combinations of protein pairs. Expression plasmid with fused N-terminal YFP fragment was co-transfected with each of all expression plasmids that fused with C-terminal YFP fragment, respectively. TPP1 and TIN2 fusion proteins were used as positive controls. Fluorescent signals were visualized under UV microscopy. In summary, several protein-protein interactions were detected, although the fluorescent signal strength varies (**Figure 4. & Table 4.**).

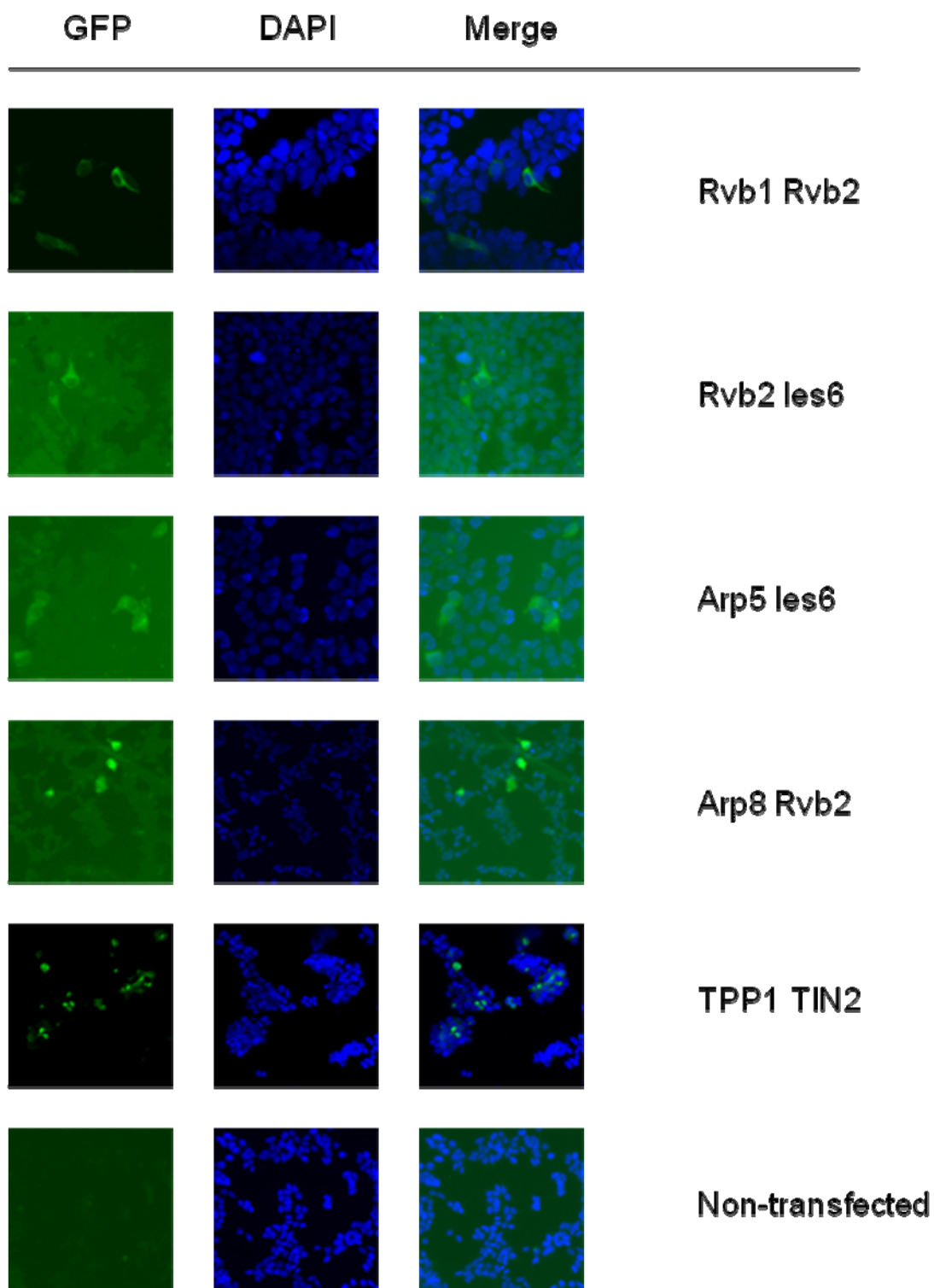


Figure 4. Fluorescent microscopy of BiFC assay. INO80 complex subunits were tagged with either C- or N-terminal YFP fragment, and co-transfected with subunits fused to complementary YFP fragment. Cells transfected with TPP1 & TIN2 were used as positive control and non-transfected HEK293 cells were served as negative control.

	Rvb1	Rvb2	les2	les6	Arp4	Arp5	Arp8
Rvb1		+++	-	-	-	-	-
Rvb2			-	+	-	-	+
les2				-	-	-	-
les6					-	+	-
Arp4						-	-
Arp5							-
Arp8							

Table 4. Summary of protein-protein interactions among INO80 complex subunits identified by BiFC assay.

Discussion

The architectures of both yeast and human INO80 complex remain poorly understood. Data from tandem affinity purification assays (Molecular Interactions Database, <http://mint.bio.uniroma2.it/mint/Welcome.do>) suggests that yeast Arp4, Arp5, Arp8, Rvb1, Rvb2, les2 and les6 have direct interactions with each other. However, affinity purifications may not represent real situations in cellular environment. Furthermore, although highly conserved, human INO80 complex may not share the same structural features with that of the lower eukaryotes.

From several duplicated experiments, I was able to detect interactions between Rvb1-Rvb2, les6-Rvb2, Arp8-Rvb2 and Arp5-les6. As expected, among all detectable interactions, the Rvb1-Rvb2 pair exhibits the highest signal strength. This phenomenon may simply due to the relatively higher concentration of Rvb1-Rvb2 subunit, which has a 6-fold stoichiometry against Ino80 in IP assay and also presents in other complex (137). Surprisingly, all interactions between INO80 components were detected both in cytoplasm and nucleus. It indicates that the INO80 complex may also present in cytoplasm. However, the immunostaining of Ino80 protein from Dr. Shen Xuetong and our labs suggested nuclear localization of this protein (131, Data not shown). Moreover, although the cytoplasmic localization of Rvb1/Rvb2 has been reported previously (145, 146), the function of cytoplasmic Rvbs remains unknown.

At the same time, I was unable to detect fluorescent signals among 3 Actin-related proteins, namely, Arp4, Arp5 and Arp8. It is possible that the impacted INO80 complex structure prevents reassembling of YPF fragments. It is also possible, however, that Arp proteins may not interact with each other directly. Previous studies have revealed that Ino80 contains docking sites for Actin, Arps, Rvbs and les subunits. Thus, Arp4, Arp5 and Arp8 proteins may interact directly with Ino80 and Actin. To further dissect structure of INO80 complex and reveal its localization in vivo, it is necessary to develop BiFC constructs of Ino80 and Actin.

Another potential factor affecting the BiFC assay is its sensitivity of detection. The interactions listed in Table 4 are detected by eye under microscope, which is limited by the sensitivity of human vision. It is possible that there are weak interactions or interactions that do not allow an perfect structural reconstitution of the YFG protein. In such a case, certain protein protein interactions may be undetectable by visual analysis. It may require flow cytometry to carry out further and more quantitative analysis.

Bibliography

121. Saha A, Wittmeyer J, Cairns BR. Chromatin remodelling: the industrial revolution of DNA around histones. *Nat Rev Mol Cell Biol* 2006;7:437-47.
122. Jin J, Cai Y, Li B, et al. In and out: histone variant exchange in chromatin. *Trends Biochem Sci* 2005;30:680-7.
123. Flaus A, Martin DM, Barton GJ, Owen-Hughes T. Identification of multiple distinct Snf2 subfamilies with conserved structural motifs. *Nucleic Acids Res* 2006;34:2887-905.
124. Conaway RC, Conaway JW. The INO80 chromatin remodeling complex in transcription, replication and repair. *Trends Biochem Sci* 2009;34:71-7.
125. Ebbert R, Birkmann A, Schuller H-J. The product of the SNF2/SWI2 paralogue INO80 of *Saccharomyces cerevisiae* required for efficient expression of various yeast structural genes is part of a high-molecular-weight protein complex. *Molecular Microbiology* 1999;32:741-51.
126. Shimada K, Oma Y, Schleker T, et al. Ino80 chromatin remodeling complex promotes recovery of stalled replication forks. *Curr Biol* 2008;18:566-75.
127. Fritsch O, Benvenuto G, Bowler C, Molinier J, Hohn B. The INO80 protein controls homologous recombination in *Arabidopsis thaliana*. *Mol Cell* 2004;16:479-85.
128. Cai Y, Jin J, Yao T, et al. YY1 functions with INO80 to activate transcription. *Nat Struct Mol Biol* 2007;14:872-4.
129. Papamichos-Chronakis M, Peterson CL. The Ino80 chromatin-remodeling enzyme regulates replisome function and stability. *Nat Struct Mol Biol* 2008;15:338-45.

130. Vincent JA, Kwong TJ, Tsukiyama T. ATP-dependent chromatin remodeling shapes the DNA replication landscape. *Nat Struct Mol Biol* 2008;15:477-84.
131. Shen X, Mizuguchi G, Hamiche A, Wu C. A chromatin remodelling complex involved in transcription and DNA processing. *Nature* 2000;406:541-4.
132. Wu S, Shi Y, Mulligan P, et al. A YY1-INO80 complex regulates genomic stability through homologous recombination-based repair. *Nat Struct Mol Biol* 2007;14:1165-72.
133. van Attikum H, Fritsch O, Hohn B, Gasser SM. Recruitment of the INO80 Complex by H2A Phosphorylation Links ATP-Dependent Chromatin Remodeling with DNA Double-Strand Break Repair. *Cell* 2004;119:777-88.
134. van Attikum H, Fritsch O, Gasser SM. Distinct roles for SWR1 and INO80 chromatin remodeling complexes at chromosomal double-strand breaks. *Embo J* 2007;26:4113-25.
135. Morrison AJ, Highland J, Krogan NJ, et al. INO80 and [gamma]-H2AX Interaction Links ATP-Dependent Chromatin Remodeling to DNA Damage Repair. *Cell* 2004;119:767-75.
136. Morrison AJ, Kim JA, Person MD, et al. Mec1/Tel1 phosphorylation of the INO80 chromatin remodeling complex influences DNA damage checkpoint responses. *Cell* 2007;130:499-511.
137. Jin J, Cai Y, Yao T, et al. A Mammalian Chromatin Remodeling Complex with Similarities to the Yeast INO80 Complex
10.1074/jbc.M509128200. *J Biol Chem* 2005;280:41207-12.
138. West SC. Processing of recombination intermediates by the RuvABC proteins. *Annu Rev Genet* 1997;31:213-44.

139. Matias PM, Gorynia S, Donner P, Carrondo MA. Crystal structure of the human AAA+ protein RuvBL1. *J Biol Chem* 2006;281:38918-29.
140. Puri T, Wendler P, Sigala B, Saibil H, Tsaneva IR. Dodecameric structure and ATPase activity of the human TIP48/TIP49 complex. *J Mol Biol* 2007;366:179-92.
141. Jonsson ZO, Jha S, Wohlschlegel JA, Dutta A. Rvb1p/Rvb2p recruit Arp5p and assemble a functional Ino80 chromatin remodeling complex. *Mol Cell* 2004;16:465-77.
142. Shen X, Ranallo R, Choi E, Wu C. Involvement of actin-related proteins in ATP-dependent chromatin remodeling. *Mol Cell* 2003;12:147-55.
143. Downs JA, Allard S, Jobin-Robitaille O, et al. Binding of chromatin-modifying activities to phosphorylated histone H2A at DNA damage sites. *Mol Cell* 2004;16:979-90.
144. Hu CD, Chinenov Y, Kerppola TK. Visualization of interactions among bZIP and Rel family proteins in living cells using bimolecular fluorescence complementation. *Mol Cell* 2002;9:789-98.
145. Salzer U, Kubicek M, Prohaska R. Isolation, molecular characterization, and tissue-specific expression of ECP-51 and ECP-54 (TIP49), two homologous, interacting erythroid cytosolic proteins. *Biochim Biophys Acta* 1999;1446:365-70.
146. Rousseau B, Menard L, Haurie V, et al. Overexpression and role of the ATPase and putative DNA helicase RuvB-like 2 in human hepatocellular carcinoma. *Hepatology* 2007;46:1108-18.

Appendix II. Data Sheets of Irradiated Mice

Table 1. Data sheet of Irradiated p53^{+/+} Mice

ID. NO.	Geno type	sex	DOB	IR received	DOD	Lifespan (wks)	COD
99	P	F	8/10/2007	9/12/2007	2/8/2008	26.1	lymphoma
107	P	M	8/19/2007	9/12/2007	3/28/2008	31.4	lymphoma
227	P	M	2/11/2008	3/26/2008	10/25/2008	36.6	unknown
225	P	M	2/11/2008	3/26/2008	11/13/2008	39.1	lymphoma
118	P	F	8/30/2007	10/18/2007	6/3/2008	39.6	lymphoma, adenocarcinoma
211	P	F	2/10/2008	3/26/2008	12/16/2008	44.1	unknown
97	P	F	8/10/2007	9/12/2007	6/23/2008	45.3	lymphoma, adenocarcinoma
105	P	F	8/19/2007	9/12/2007	7/18/2008	47.6	lymphoma, osteosarcoma
76	P	F	7/9/2007	8/20/2007	6/25/2008	50	carcinoma
94	P	F	8/4/2007	9/12/2007	8/6/2008	52.4	lymphoma, adenocarcinoma
164	P	M	10/1/2007	10/18/2007	10/10/2008	53.4	osteosarcoma
176	P	F	11/24/2008	1/29/2008	12/31/2008	57.4	sarcoma
174	P	F	11/24/2008	1/29/2008	1/6/2009	58.3	osteosarcoma
179	P	M	11/24/2008	1/29/2008	3/6/2009	66.7	unknown
100	P	M	8/10/2007	9/12/2007	12/26/2008	71.6	lymphoma
85	P	M	7/23/2007	9/3/2007	3/18/2009	N/A	N/A
92	P	M	8/5/2007	9/12/2007	3/18/2009	N/A	N/A
185	P	F	11/23/2007	1/29/2008	3/18/2009	N/A	N/A
215	P	F	2/9/2008	3/26/2008	3/18/2009	N/A	N/A
220	P	M	2/10/2008	3/26/2008	3/18/2009	N/A	N/A

P: p53^{+/+}. N/A: mice discarded by the end of experiment (3/18/2009, no tumor observed).

Table 2. Data sheet of Irradiated RMI1^{+/+}p53^{+/+} Mice

ID. NO.	Geno type	sex	DOB	IR received	DOD	Lifespan (wks)	COD
95	RP	F	8/10/2007	9/12/2007	12/31/2007	20.4	unknown
122	RP	M	8/30/2007	10/18/2007	1/29/2008	21.7	lymphoma
217	RP	F	2/11/2008	3/26/2007	7/22/2008	23.3	lymphoma (high-grade), osteosarcoma
140	RP	F	9/2/2007	10/18/2007	3/1/2008	26.1	lymphoma
218	RP	F	2/11/2007	3/26/2008	9/3/2008	29.3	lymphoma
178	RP	M	11/24/2007	1/29/2008	6/30/2008	31.4	osteosarcoma
208	RP	F	2/10/2008	3/26/2008	9/26/2008	32.7	lymphoma
79	RP	M	7/9/2007	8/20/2007	2/27/2008	33.1	unknown
117	RP	F	8/30/2007	10/8/2007	4/25/2008	34.1	unknown
228	RP	M	2/11/2008	3/26/2008	10/10/2008	34.5	carcinoma
135	RP	M	9/2/2008	10/8/2007	4/26/2008	34.6	lymphoma
77	RP	M	7/9/2007	8/20/2007	3/7/2008	34.6	osteosarcoma, sarcoma
214	RP	F	2/10/2008	3/26/2008	11/18/2008	36.9	lymphoma
223	RP	M	2/11/2008	3/26/2008	11/18/2008	37.3	lymphoma
74	RP	F	6/25/2007	8/8/2007	4/12/2008	41.9	lymphoma
96	RP	F	8/10/2007	9/12/2007	6/23/2008	45.4	carcinoma
173	RP	F	11/24/2007	1/29/2008	10/22/2008	47.6	sarcoma, lymphoma
190	RP	M	11/23/2007	1/29/2008	12/12/2008	54.9	lymphoma, adenocarcinoma
80	RP	M	7/9/2007	8/20/2007	8/20/2008	58	lymphoma
73	RP	M	6/25/2007	8/8/2007	3/18/2009	N/A	N/A
182	RP	F	11/23/2007	1/29/2007	3/18/2009	N/A	N/A
184	RP	F	11/23/2007	1/29/2007	3/18/2009	N/A	N/A
180	RP	M	11/24/2007	1/29/2007	3/18/2009	N/A	N/A

RP: RMI1^{+/+} p53^{+/+}. N/A: mice discarded by the end of experiment (3/18/2009, no tumor observed).

Table 3. Data sheet of Irradiated RMI1^{+/+} Mice

ID No.	Genotype	sex	DOB	IR received	DDP	Lifespan (days)	COD
209	R	F	2/10/2008	3/26/2008	7/15/2008	221	unknown
216	R	F	2/10/2008	3/26/2008	8/21/2008	273	lymphoma
121	R	M	8/30/2007	10/18/2007	4/12/2008	324	lymphoma
137	R	F	9/2/2007	10/18/2007	10/1/2008	55	sarcoma
101	R	M	8/10/2007	10/18/2007	10/7/2008	604	unknown
81	R	F	7/23/2007	9/3/2007	12/21/2008	736	lymphoma
139	R	F	9/2/2007	10/18/2007	3/6/2009	784	sarcoma
71	R	M	6/25/2007	8/6/2007	3/18/2009	N/A	N/A
84	R	F	7/23/2007	9/3/2007	3/18/2009	N/A	N/A
86	R	M	7/23/2007	9/3/2007	3/18/2009	N/A	N/A
87	R	M	7/23/2007	9/3/2007	3/18/2009	N/A	N/A
93	R	M	8/4/2007	9/12/2007	3/18/2009	N/A	N/A
102	R	F	8/19/2007	9/12/2007	3/18/2009	N/A	N/A
106	R	F	8/19/2007	9/12/2007	3/18/2009	N/A	N/A
115	R	M	8/19/2007	9/12/2007	3/18/2009	N/A	N/A
116	R	M	8/19/2007	9/12/2007	3/18/2009	N/A	N/A
141	R	F	9/2/2007	10/8/2007	3/18/2009	N/A	N/A
193	R	M	11/23/2008	1/29/2008	3/18/2009	N/A	N/A
189	R	M	11/23/2008	1/29/2008	3/18/2009	N/A	N/A
177	R	M	11/24/2008	1/29/2008	3/18/2009	N/A	N/A
210	R	F	2/10/2008	3/26/2008	3/18/2009	N/A	N/A
226	R	M	2/11/2008	3/26/2008	3/18/2009	N/A	N/A
227	R	M	2/11/2008	3/26/2008	3/18/2009	N/A	N/A

R: RMI1^{+/+}. N/A: mice discarded by the end of experiment (3/18/2009, no tumor observed).

Table 4. Data sheet of Irradiated Wild Type Mice

ID. NO.	Geno type	sex	DOB	IR received	DOD	Lifespan (wks)	COD
75	WT	M	6/25/2007	8/6/2007	1/29/2008	26.7	lymphoma
136	WT	F	9/2/2007	10/18/2007	5/27/2008	38.3	lymphoma
219	WT	F	2/10/2008	3/26/2008	1/16/2009	49.6	lymphoma
188	WT	M	11/23/2007	1/29/2008	12/12/2008	54.9	lymphoma, sarcoma
72	WT	M	6/25/2007	8/6/2007	7/27/2008	56.7	unknown
119	WT	F	8/30/2007	10/18/2007	10/7/2008	57.6	lymphoma
138	WT	F	9/2/2007	10/18/2007	12/8/2008	66	lymphoma
114	WT	M	8/19/2007	10/18/2007	12/12/2008	66.6	lymphoma
124	WT	M	8/30/2007	10/8/2007	1/29/2009	73.9	lymphoma, agiosarcoma
78	WT	M	7/9/2007	8/20/2007	3/18/2009	N/A	N/A
83	WT	F	7/23/2007	9/3/2007	3/18/2009	N/A	N/A
82	WT	F	7/23/2007	9/3/2007	3/18/2009	N/A	N/A
104	WT	F	8/19/2007	9/12/2007	3/18/2009	N/A	N/A
120	WT	F	8/30/2007	10/8/2007	3/18/2009	N/A	N/A
125	WT	M	8/30/2007	10/8/2007	3/18/2009	N/A	N/A
123	WT	M	8/30/2007	10/8/2007	3/18/2009	N/A	N/A
134	WT	M	9/2/2007	10/8/2007	3/18/2009	N/A	N/A
142	WT	F	9/2/2007	10/8/2007	3/18/2009	N/A	N/A
191	WT	M	11/23/2007	1/29/2008	3/18/2009	N/A	N/A
186	WT	F	11/23/2007	1/29/2008	3/18/2009	N/A	N/A
183	WT	F	11/23/2007	1/29/2008	3/18/2009	N/A	N/A
187	WT	M	11/23/2007	1/29/2008	3/18/2009	N/A	N/A
188	WT	M	11/23/2007	1/29/2008	3/18/2009	N/A	N/A
175	WT	F	11/24/2007	1/29/2008	3/18/2009	N/A	N/A
181	WT	M	11/24/2007	1/29/2008	3/18/2009	N/A	N/A
213	WT	F	2/9/2008	3/26/2008	3/18/2009	N/A	N/A
222	WT	M	2/10/2008	3/26/2008	3/18/2009	N/A	N/A
221	WT	M	2/10/2008	3/26/2008	3/18/2009	N/A	N/A

WT: wild type . N/A: mice discarded by the end of experiment (3/18/2009, no tumor observed.

VITA

Haoyi Chen were born in Shanghai, China in 1979, the son of Yizheng Chen and Aihua Li. In 1998, he entered School of Biological Sciences of Fudan University and graduated with a Bachelor degree of Science in Biology 4 years later. In August, 2002, he came to United States and was enrolled as graduate student in Department of Biological Sciences, Bowling Green State University. One year later, he transferred to University of Texas, Graduate School of Biomedical Sciences and joined Dr. Lei Li's laboratory in the University of Texas M.D. Anderson Cancer Center.